R. & M. No. 3601

R. & M. No. 3601

MINISTRY OF TECHNOLOGY

AERONAUTICAL RESEARCH COUNCIL
REPORTS AND MEMORANDA

Performance Characteristics and Methods of Testing of Force-Feedback Accelerometers

By I. L. THOMAS and R. H. EVANS

I.E.E. Dept., R.A.E., Farnborough

LONDON: HER MAJESTY'S STATIONERY OFFICE
1969
PRICE £1 7*s*. 6*d*. NET

Performance Characteristics and Methods of Testing of Force-Feedback Accelerometers

By I. L. THOMAS and R. H. EVANS

I.E.E. Dept., R.A.E., Farnborough

Reports and Memoranda No. 3601*
August, 1967

Summary.

The more important parameters of force-feedback accelerometers are defined, sources of error are discussed and an outline is given of methods by which the accelerometers may be evaluated and calibrated. The emphasis is on treating the accelerometer as a self-contained component rather than as part of a navigation or other system. It is hoped that sufficient information on static and dynamic performance is included to be of value to a wide range of potential users as well as those concerned with the instruments in a more specialised capacity.

This Report is an updated and expanded version of R.A.E. Technical Note IAP 1076 published in 1960. The new material mainly concerns the viscous damped (oil-filled) type of accelerometer and a more extended treatment of the dynamic response of both air-filled and oil-filled instruments.

LIST OF CONTENTS

*Replaces RAE Technical Report 67 183 (A.R.C. 30 615).

LIST OF CONTENTS—*continued*

1. *Introduction.*

Force-feedback accelerometers operate by measuring the inertial forces acting upon a mass when it is subjected to acceleration. They were originally developed principally for inertial guidance and navigation applications in aircraft and missiles and are in widespread use for this purpose. However, their high accuracy and reasonably wide frequency response make them suitable for other applications such as aircraft flight test work.

The aim of this Report is to define the more important parameters and sources of error found in precision accelerometers and to outline some of the methods by which accelerometers may be calibrated. It is hoped that sufficient information on static and dynamic performance is included to be of value to a wide range of potential users as well as those concerned with the instruments in a more specialised capacity. A high proportion of the information has been published in a previous R.A.E. Technical Note[1] (dated 1960) but it is thought worth-while to bring the information up to date and to expand certain topics.

After a brief description of the principles of operation, the main parameters are defined and there follows a discussion of the main error sources, the discussion being divided into three parts dealing respectively with errors common to all varieties and errors peculiar to two particular methods of suspending the proof mass. Methods of testing under both static and dynamic conditions are then described, followed by further comments on the dynamic performance. In particular a comparison is made between the dynamic characteristics of air-filled and oil-filled accelerometers.

The general discussion is backed by a more detailed mathematical analysis in Appendices A and C, dealing respectively with the static-force balance equations and the dynamic response. It may be helpful to refer to these Appendices when reading the main body of the report, especially Sections 3, 4 and 7. Appendix D gives some typical tests results which illustrate the order of magnitude of the errors.

2. *Principles of Operation.*

2.1. *General Principles.*

There are two main types of precision accelerometers working on the force-feedback principle, differing in the method of suspending the proof mass. They are the pivoted arm type and the rectilinear type, schematic diagrams of which are shown in Fig. 1. The former type may employ a pivot and jewelled bearing but for the highest precision a spring hinge is employed and this is the type illustrated. The pivoted arm type employing a spring hinge is easily the most common type amongst high precision accelerometers. Instruments have also been designed, using one or other of these suspension methods, such that acceleration may be measured simultaneously along two mutually perpendicular axes. Most of the considerations discussed in this Report apply to each axis of such multi-axis instruments, but it is not proposed to deal with the specific properties of the multi-axis configuration.

Basically, accelerometers of the force-feedback type measure the acceleration of a vehicle by measuring the force needed to constrain a proof mass to move with the vehicle or, in other words, the force needed to prevent the mass moving relative to the instrument frame. Some form of pick-off produces a signal proportional to relative movement of the mass and frame and this signal is amplified and used to produce a direct current in a coil mounted on the mass. The interaction of this current with a permanent magnet field provides the required restoring force. Ideally, therefore, this current is proportional to the acceleration along the direction in which the mass is free to move and is the output quantity of the accelerometer.

A typical circuit for a pivoted arm type of accelerometer is shown in Fig. 2. The excitation coils are supplied with A.C. of frequency usually in the range 4 kc/s to 20 kc/s, and a pick-off coil is attached near the free end of the arm. The feedback amplifier has an A.C. section, a phase-sensitive rectifier (demodulator) and a D.C. section. The final displacement of the proof-mass under the action of acceleration can be made very small (e.g. one arc sec per g) by making the amplifier gain sufficiently high. Under such conditions the accuracy of the restoring current as a measure of acceleration is dependent (to a first order) only on the constancy of the magnet flux embracing the coil and the constancy of the mass itself. Usually the current is converted to a proportional voltage by means of a precision readout resistor.

Note. To avoid confusion the symbol 'gm' has been used for grammes and the symbol 'g' for the unit of acceleration due to gravity (approximately 981 cm/sec^2).

Various modifications of the basic circuit are possible. For example, the feedback loop may contain a pulse generator giving positive and negative pulses; the restoring current is then of a pulsed nature rather than D.C., thus facilitating operation in conjunction with digital equipment. Of course, the restoring current may be maintained as D.C. but the final output digitised by means of digital voltmeters or digital milliammeters. Another possibility for navigation is to preserve analogue operation throughout but to modify the feedback circuit so that the output voltage is an analogue measure of velocity i.e. an integration has been achieved within the loop[2].

Various R.A.E. reports have been issued assessing the performance of typical air-filled[3] and oil-filled[4,5] accelerometers.

2.2. *Stabilisation of the Loop.*

The accelerometer with its associated amplifier forms a closed-loop servo system of high loop gain and will be unstable unless a stabilising network is included in the amplifier. For example, a phase-advance network may be inserted after the demodulator as shown in Fig. 2. Alternatively, the loop may be damped mechanically by filling the accelerometer with a suitable oil and hermetically sealed. An advantage of oil filling is that the amplifier is smaller because of the absence of the stabilising network; this is particularly significant with the modern use of solid state integrated circuits for the amplifier because the stabilising network does not readilly lend itself to this technique and it is likely therefore to be disproportionately large. Further, the performance of the accelerometer in the presence of vibration is better because the oil introduces a greater degree of damping than can readilly be achieved with electrical networks; in fact with oil filling there is usually no resonant peak in the frequency response. Moreover, this improved damping can be achieved even with a higher loop gain, and hence a smaller arm deflection, than is permissible with the unfilled type. On the other hand, the processes of vacuum pumping, oil filling and hermetic sealing add considerably to the complications of manufacture. Also, accelerometers of the oil filled type usually have to be operated at a controlled temperature in order to maintain satisfactory values of density and viscosity of the oil. In general, the oil-filled type would be employed where it was essential to take advantage of its particular properties and especially where a temperature controlled environment had to be provided in any case (e.g. for other instruments).

2.3. *Pick-offs.*

In an alternative form of electro-magnetic pick-off, there are four fixed excitation coils connected in a bridge and the coil at the end of the arm is replaced by a spade-shaped piece of metal which effectively acts as a shorted turn whose coupling with the coils varies with the position of the arm, hence unbalancing the bridge. The remainder of the circuit is the same as for the moving coil pick-off. The shorted-turn type of pick-off gives a simpler construction, including the elimination of two electrical connections to the moving arm. It is usual for one side of the amplifier input, that is, one side of the pick-off output to be earthed; this means that an assembly of shorted-turn accelerometers has the disadvantage of demanding a separate isolated excitation supply from each instrument. Various alternative arrangements are possible to overcome this difficulty. For example, the four coils may be connected in pairs to form the primary and secondary winding of a transformer and the position of the spade alters the coupling of the windings and hence the output of the secondary. The performance of eddy-current (shorted-turn) pick-offs for accelerometers had been investigated by Appleton[6].

Capacitative pick-offs have also been used in some precision force-feedback accelerometers. With these, a pre-amplifier must be mounted on or very close to the accelerometer because of the very high impedances in the capacity bridge.

3. *Definitions.*

3.1. *Mounting Face and Sensitive Axis.*

In inertial navigation systems an accelerometer is used to measure the acceleration along an axis which must be located to a high degree of accuracy. It is usual, therefore, for the manufacturer to provide the instrument with an accurately machined mounting face and to *define the nominal sensitive axis as being*

the normal to this face. In general it will be found that there is a fairly constant misalignment between the sensitive axis as defined above and that which becomes apparent when tests are made to determine the actual axis along which the instrument is most sensitive to accelerations. The latter is referred to as the *true sensitive axis.*

3.2. *Axis Error.*

This misalignment mentioned above is known as the *axis error* and can arise from a number of different sources, the most obvious one being the manufacturing tolerances in assembling the instrument accurately relative to the mounting face. When an axis error is present the accelerometer will be sensitive to a small extent to accelerations in the plane of the mounting face.

Axis error is therefore defined as the angle between the normal to the mounting face and the normal to the plane in which an acceleration produces no change of output.

Appendix A, equation (A.4) shows the form in which axis error affects the output of the accelerometer, and the various sources which give rise to the error.

3.3. *Range.*

The range of an accelerometer is the total acceleration which it will measure with the specified accuracy in each direction along the sensitive axis. It is usual for this to be stated in units of gravity acceleration (g's) e.g. the range of an accelerometer might be -5 g to $+12$ g.

It should be noted that the effective range may be reduced in practice by the presence of vibration, the extent of the reduction depending upon the frequency of the vibration. Suppose for example that the range was limited by amplifier saturation to ± 20 g. Then in the presence of 5 g peak vibration of frequency well below the resonant frequency of the loop, the effective range for steady acceleration would be ± 15 g. If the loop was lightly damped and had a magnification factor of 2, then in the presence of 5 g vibration near the loop resonant frequency the effective range would be reduced to ± 10 g. At higher vibration frequencies the effective range would regain its full value of ± 20 g.

3.4. *Scale Factor.*

The output quantity of accelerometers of the force-feedback type is the current flowing in the force-coil circuit, and this is, ideally, proportional to the acceleration along the true sensitive axis (*see* equations A.1 to A.4 of Appendix A). The scale factor of the instrument is therefore quoted in terms of force-coil current per unit acceleration, e.g. milliamps per g. Since the value of g varies with geographical position then any statement of scale factor must be accompanied by a note of the location in which the calibration test was made. It is unlikely that the output will be exactly proportional to the applied acceleration over the full range, and in order to obtain a value which is easily checked the scale factor quoted should be that which refers to the section of the range from -1 g to $+$ 1 g.

The scale factor is therefore defined as half of the algebraic difference of the output currents for accelerations of $+1$ g and -1 g along the true sensitive axis; the value of gravity being stated for the place where the test was carried out.

Ideally the output characteristic of an accelerometer would be of the form

$$I = Bf.$$

Actually it is more likely to be of the form

$$I = A + Bf + Cf^2 + Df^3 + \ldots\ldots$$

where A, B, C and D are constants and f is the acceleration along the sensitive axis (say in 'g' units). Hence when scale factor is determined in accordance with the definition in the preceding paragraph the actual value obtained will be $(B + D)$ and not the ideal value B.

The point is relevant to the discussion of lineaity errors in Section 3.6 where scale factor is used to set up the ideal characteristic giving

$$I = (B+D)f \text{ instead of } I = Bf.$$

It does not appear that the difference will be very great, since it seems that the major contribution to non-linearity is provided by the term Cf^2 for both types of instrument discussed.

For some specific applications it may be more advantageous to adjust the inertial navigator or other equipment on the basis of some other scale factor, e.g. one which best covers the expected operating range with minimum error. In such cases this scale factor should be quoted separately and in addition to the one defined above.

Equations (A.1) and (A.8) of Appendix A show that the scale factor depends primarily on the proof mass M and the restoring force per unit current of the restoring coil (K_c) with small corrections depending upon spring stiffness or ligament tension coupled with amplifier gain.

3.5. *Bias Force.*

Force-feedback accelerometers operate with a high loop gain which tends to hold the sensitive element in a constant position relative to the frame. Every attempt is made to ensure that no residual forces (e.g. due to spring hinge or electrical ligaments) act on the element in this position, but this can never be perfectly achieved.

Bias force is therefore defined as the output of the accelerometer when no acceleration forces are acting. Equation (A.3) of Appendix A shows what this force comprises for the two designs (for the rectilinear type, nT is to be substituted for S). The force 'b' may be considered as arising from a spring which is so weak that its rate may be neglected, but with its free position so far deflected that a significant constant effect occurs over the working range of the instrument. The other terms are due to the spring rates (S and T), and the angles through which these springs are deflected. Electrostatic or unwanted electromagnetic effects can give rise to forces of a spring-like nature but these will, in general, be non-linear, and the design should ensure that such effects are small.

3.6. *Linearity.*

This term is used to indicate the magnitude of the errors over the full range and can be expressed in a number of different ways. The definition adopted here is that the *linearity error is the difference between the actual output (after correcting for bias force and axis error) and the ideal output; this difference being expressed as a fraction of the latter. The ideal output must be taken as that obtained by multiplying the acceleration along the sensitive axis by the scale factor.*

Just as there may be a more advantageous definition of scale factor for a particular system, so there can be an alternative definition of linearity errors i.e. obtained from the best scale factor rather than from the $+1\,g$ to $-1\,g$ scale factor. These optimistic linearity figures should be treated with caution since it may be quite difficult to ensure that the equipment is, in fact, adjusted to the required scale e.g. a check test at $+1\,g$ and $-1\,g$ may be simple but to confirm readings at say $+12\,g$ and $-12\,g$ would be quite difficult.

3.6.1. *Bias discrepancy.* A convenient practical test of a force-feedback accelerometer is to measure the output at four selected positions when it is rotated in the earth's gravitational field. The four positions are (a) the two positions 180 deg. apart in which the nominal sensitive axis is parallel with the gravity vector, and (b) the two positions in which the nominal sensitive axis is perpendicular to the gravity vector.

By reference to equation (A.1) of Appendix A it will be seen that the two outputs measured under conditions (a) above can yield values for the scale factor and bias force and under conditions (b) they will give values for axis error and bias force. Under ideal conditions these two values of bias force would be identical; but if the accelerometer has a non-linear characteristic of the type shown in Fig. 3c this will not be so and the difference between the two bias values will be a function of the non-linearity. This value, known as *bias discrepancy*, is therefore a very useful parameter which is relatively easily measured.

It is shown later in Section 4.1.1(b) that the particular forms of non-linearity (error terms which are proportional to *even* powers of applied acceleration) which give rise to bias discrepancy are those which can be expected in force-feedback accelerometers. If errors proportional to the odd powers of applied acceleration are present, they will not be shown by bias discrepancy nor will they cause rectification of vibration errors.

3.7. *Cross Coupling.*

This term is used to express the fact that under certain conditions the presence of an acceleration at right angles to the true sensitive axis can cause errors of output. It is shown in Appendix A that this effect is not present to a first order in the parallel motion type as long as the ligaments remain under tension. For the pivoted arm type the effect is due to the presence of the term $M\,Cg/G$ in the denominator of equation (A.1) and the error (measured in g's) is given by equation (A.7) as

$$\delta_c \times N \times C.$$

Hence the cross coupling effect depends upon the cross acceleration (C) and the angle moved through by the arm due to the active acceleration (N). *The quantity* $\delta_c = Mg/K_c\,G$ *is therefore taken as the cross coupling coefficient and is equivalent to the angle, in radians, moved through by the arm for an acceleration of* 1 *g along the sensitive axis.*

The cross coupling effect has a particular significance when an accelerometer is subject to vibration in that rectification of the alternating force can occur. This is discussed in Sections 4.2.3 and 4.3.2.

4. *Sources of Error.*

4.1. *Errors Common to both Types of Accelerometer.*

(a) *Stability of magnets.*

Accelerometers of the force-feedback type, using a coil and magnet system to generate the restoring force are inherently dependent upon the constancy of the field strength produced in the magnet gap (K_c in equation (A.1) and (A.8) is proportional to field strength). It is well known that magnets used in high quality electrical instruments remain constant to about 1 part in 1000 over a period of several years, but this is only so if the instrument is treated carefully under laboratory conditions.

Probably one of the best indications of magnetic stability available is derived from long term tests on the accelerometers themselves. Under laboratory conditions changes of less than 1 part in 10 000 over a period of 12 months have been observed in some cases but on other instruments changes an order of magnitude greater than this have been observed. Typically, specifications set a limit of 1 part in 10 000 per month for steady drift rate of scale factor, the test usually taking place over a period of 4 months.

(b) *Demagnetizing effect of force coil.*

The passage of current through the force coil will tend to change the magnet flux linked with the coil. If the magnet has been properly aged no permanent change in flux should result from this effect for currents within the range of the instrument. Since however the passage of current through the coil in one direction tends to increase the flux, and in the opposite direction to decrease it, it follows that the accelerometer characteristic relating applied acceleration and force-coil current will tend to depart from the desirable straight line passing through the origin, i.e. a form of non-linearity appears.

It is a general practice in the design of these accelerometers to use a symmetrical system of two magnets and two foce coils, the coils being connected in series. Since in such a system the individual forces developed by each coil must be additive, it follows that when the current in one coil tends to increase its magnet flux, that in the other tends to decrease it. Assuming that, over the small range involved, the effect is linear, conditions may be represented by the diagram of Fig. 3a, for a symmetrical system. It is evident that such a system is self-compensating for this effect, and what may be called the average flux for the whole system does not vary with force-coil current. No distortion of the accelerometer characteristic should therefore result.

If however, due to some lack of symmetry, conditions are as in Fig. 3b, in which the individual characteristics are of different slopes, the average flux will now vary with coil current and the accelerometer characteristic will be distorted.

To a first approximation, for a coil current I we have:

$$\text{average flux } \Phi_{I=I} = \Phi_{I=0} \pm \text{const.} \times I .$$

$$\text{Therefore force produced by system} = I(\Phi_{I=0} + \text{const.} \times I)$$

$$= I\,\Phi_{I=0} + \text{const.}\, I^2 .$$

The term $\Phi_{I=0}\, I$ represents the ideal straight-line through the origin. The effect of the lack of symmetry is therefore to produce an error proportional to the square of the applied acceleration. The resulting accelerometer characteristic would therefore be of the form indicated in Fig. 3c and the four-position test mentioned earlier would show a large value for bias discrepancy. Tests on a precision centrifuge in the range approximately $\pm 10\,g$ have in fact confirmed that the predominant non-linearity is of this quadratic form.

The fact that the errors tend to obey a square law indicates that the effect becomes more important at high accelerations.

If an accelerometer with such a characteristic is subjected to an acceleration which is varying sinusoidally, the waveform of the force-coil current will obviously be distorted, the two halves of the wave being of different amplitude. Thus although the average value of the acceleration is zero, the average value of the current will not be zero. Such an accelerometer operating with a component of vibration acting in the direction of its sensitive axis can therefore be expected to develop errors. The long-stroke vibrator mentioned in Section 6.3 makes use of this property to measure the non-linearity.

Reference has been made, in Section 2, to a particular type of accelerometer having the pendulous arm carried by a spring hinge. For this type of instrument it was found fairly easy to reduce lack of symmetry by inserting shims between one or other magnet and its mounting face on the body of the instrument. Speaking approximately, a movement of 0·005 inch of the magnet altered the bias discrepancy by about 1 part in 10^4 of 1 g. A small change of similar order appeared in scale factor. The direction of the change in bias discrepancy obviously depends on which magnet is moved.

A possible alternative is to provide armature reaction compensating coils wound on the magnets, carrying the whole or a fixed proportion of the force-coil current. Such a device would of course have to be adopted at the design stage of the instrument.

(c) *Constancy of magnetic field over full range.*

If an accelerometer is to have a linear relationship of output *versus* acceleration then the effective field should be constant over the operational range of movement of the force coil, (i.e. K_c remains constant). It is possible to approach this requirement in two ways: (a) by making the coil uniform and wide enough to embrace the majority of the leakage field and (b) by making the coil narrow so that no part of it ever moves out of the central uniform field (Fig. 4). The first of these methods has the serious disadvantage that the large coils add considerable superflous weight to the sensitive element. For the second method the magnet material is not used economically but this is usually not a serious disadvantage. In either case improvement results from keeping the loop gain high, i.e. reducing the total range of coil movement.

The effect of a non-uniform field on the performance of the accelerometer is to introduce linearity errors particularly towards the extremes of the range of operation.

For an accelerometer of high accuracy the coil movement per g of applied acceleration is very small, i.e. 10 micro-inches per g is typical. This means that it is not difficult to ensure that the field is constant over the operational movement of the coil.

An effect which can be larger than the above is the expansion of the coil due to self heating at high acceleration levels. At say 10 g the power dissipated in the small coil may be more than 1 watt giving a temperature rise of up to 100 deg. C. The effective movement of the coil due to expansion can then

approach 0·001 inch, i.e. 10 times the movement due directly to the applied acceleration. It has been shown that it is possible to arrange the coil dimensions and its position in the magnet gap so that expansion causes no significant change of effective field strength. Also, in practice, the full temperature rise rarely occurs, since high acceleration cannot be maintained for long periods of time, except under very severe vibration.

(d) *Drift of pick-off null point.*

If for any reason such as mechanical instability or changes in the electrical or magnetic components, the zero of the pick-off moves to a new position then the calibration of the accelerometer will be altered. In the case of the pivoted arm (spring hinge) type two main effects are introduced. Firstly, there is a change of axis error equal to the angle through which the arm has to deflect to reach the new null position; and secondly the bias force is changed by an amount which depends primarily on the stiffness of the spring hinge. These effects are illustrated by changes in α and ρ in equation (A.1) of Appendix A. In the case of the rectilinear type, no change of axis error will result but there will be a change of bias force which may be large if the ligament tension is high. This is shown by a change of ρ in equation (A.8). If the magnet field is not uniform then changes of scale factor and linearity will also be introduced.

(e) *Loop stability.*

As previously mentioned the accelerometer with its associated amplifier comprises a closed loop servo system with a fairly high loop gain or stiffness (*see* Appendix C). It may, therefore, have a tendency to become underdamped or actually unstable for small changes in operating conditions. The effect of insufficient damping will be to give rise to large errors or complete failure when subjected to vibration. If the system actually becomes unstable the sensitive element will vibrate against its limit stops and permanent damage is likely to result.

In common with other types of servo systems for aircraft or missile use the performance should be satisfactory if the phase margin is about 30 deg. and the gain margin at least 6 db.

(f) *Changes of amplifier gain and balance.*

The output stage of an accelerometer amplifier is, of necessity, d.c. connected and therefore drift of transistor characteristics will cause an output current to flow when no input signal is present (I_u). This unbalance of the amplifier is to some extent equivalent to a drift of the pick-off null, since the sensitive element must now rest in a different position for zero output. This is shown by the grouping of the terms in equations (A.1) and (A.8). Changes of axis error and bias force will therefore occur with changes of amplifier balance. A second effect of this is that the operating range of the instrument will be unsymmetrical by the amount of the unbalance current and this may limit the range of operation in one direction and may cause rectification of vibrational accelerations.

Changes of the gain (G) of the amplifier will also introduce errors due to the increased (or decreased) movement of the sensitive element for a given acceleration, although an increase of gain may cause oscillation before any significant errors become evident. Considering the more likely case of a decrease of gain, then for a given applied acceleration the sensitive element movement will be greater, and greater spring forces will arise. The effect is shown by equations (A.1) and (A.8) to result primarily in a small change in the scale factor depending upon the extent of the change in G and the magnitude of the spring forces or ligament tensions.

If the drop in gain is large then further errors will be introduced due to the increased movement carrying the operating point into regions where the field strength may be different or where the non-linearities of the spring forces may be significant. Also the increased movement will increase the cross coupling co-efficient proportionately.

(g) *Quadrature component of pick-off voltage.*

Because the amplifier contains a phase-sensitive rectifier (demodulator) which is energised by the same voltage source as the accelerometer excitation, the loop effectively operates only on the in-phase

component of the pick-off voltage. It is found however that the pick-off output usually contains not only the in-phase signal proportional to displacement but also a quadrature output which is substantially constant and exists even at the null position. In fact the quadrature component may simply be taken to be the pick-off output which is present when the accelerometer is in the zero-g position, and it is therefore easily measured. Although not of direct consequence in the operation of the loop, the quadrature component must be controlled because an excessive amount will tend to saturate the amplifier and drive it into non-linear regions, as well as producing excessive ripple across the readout resistance to the possible detriment of the following circuits or measuring instruments.

In some designs of pick-off there is a phase shift between the true signal and the excitation; this may be compensated by an equal and opposite shift built into the amplifier, or sometimes by tuning the pick-off with a capacitor. In any case, the quadrature component discussed above is still the pick-off voltage present at zero g.

(h) *Temperature rise in normal operation.*

For the intended applications of these accelerometers, accelerations of magnitude of the extreme of the range should occur only for short periods. Advantage has been taken of this to design the force-coils with a short time-rating for self-heating. Hence when subjected to high accelerations, the temperature of the force-coils rises rather rapidly, setting up temperature gradients in the instrument. The following effects may result from this.

(i) The effective magnet flux may be disturbed. It is usual to provide the magnets with temperature-sensitive magnetic shunts adjusted to compensate for the temperature-produced change of flux of the magnet materials. This adjustment will obviously be made for steady-state conditions, and will be incomplete if a temperature gradient appears across the magnet. Thus the scale factor of the instrument might be expected to change under sustained high accelerations, producing non-linearity.

(ii) The force coil will expand and embrace more flux, again leading to the appearance of linearity errors.

(iii) Uneven heating of the arm of the pivoted arm type may lead to slight distortion causing displacement of the pick-off null and thence to changes in bias force.

4.1.2. *Effects due to environment.*

(a) *Temperature.*

The major effect of temperature change on this type of accelerometer is to change the magnet field strength; this causes a change in K_c and therefore alters the scale factor. For an uncompensated magnet a typical temperature coefficient would be about 0·02 per cent to 0·03 per cent per deg. C, but with compensation by a temperature sensitive magnetic shunt this can be reduced by a large factor over a limited range and by a useful factor over quite a wide range (e.g. a typical specification would call for a temperature coefficient of scale factor not exceeding 0·005 per cent per deg. C over the range 20 deg. C to 65 deg. C). An alternative method of correction is to fit some form of temperature sensing element onto the magnet and use this to control a correction term applied at any convenient point in the circuit. For example, this signal could be used after amplification to pass current through a fixed coil on the magnet to compensate directly for the change of field strength. Alternatively the temperature sensing element could be a resistance mounted inside the instrument but forming part of a series/parallel readout circuit designed so that the final readout voltage, although not the accelerometer as such, is temperature compensated—this method is particularly good for compensation over a wide temperature range. A discussion of temperature-compensation methods is given in Ref. 7.

There are many other small effects brought about by changes of temperature such as dimensional changes affecting the pick-off null and changes in spring rates or ligament tensions. The magnitude of these effects depends critically upon the detail of the design of any particular accelerometer.

It is usual for an accelerometer to be designed to give its highest accuracy over a particular and limited range of temperature, but it should be capable of operating to a lower accuracy standard over a much wider range.

When mounting an accelerometer care should be taken to ensure that the heat required to maintain it at its operating temperature is supplied in a symmetrical manner, because a one-sided application of heat can cause temperature gradients leading to errors. Many of the effects would be the same as those resulting from self-heating, as described in Section 4.1.1(h) above. Because of aircraft rapid-readiness requirements, accelerometers are sometimes warmed up rapidly from cold to operating temperature and are expected to have a stable output suitable for navigator alignment within a few minutes of switch-on. Temperature-gradient effects probably predominate in these circumstances and special laboratory tests have been devised to measure how the accelerometer output settles to its final value under warm-up conditions designed to simulate those encountered in practice.

(b) *Vibration.*

Accelerometers of the types under consideration are often intended for use in applications where the vibration conditions may be severe. Fig. 5 shows a vibration specification for a particular application with one area in which the accelerometer must operate with full accuracy, and an extended area in which the errors may build up to relatively large values but the accelerometer must not sustain permanent damage. A more typical aircraft vibration spectrum is shown in Fig. 6.

The principal effects of vibration are as follows.

(i) When the vibration is directed along the sensitive axis, any non-linearity terms in the output characteristics represented by even powers of acceleration will rectify and cause errors. As shown in Section 4.1.1(b) it is even powers (especially a square term) which are most likely to be present, due to the effect of armature reaction. The magnitude of the effect can be predicted from the value of bias discrepancy measured in the static ± 1 g tests (Section 3.6.1). A method of measuring the non-linearity effect at low frequencies and at amplitudes greater than 1 g is the long-stroke vibrator (Section 6.3).

(ii) For large amplitudes of vibration along the sensitive axis, especially near the resonant frequency of the loop, non-linearity errors additional to those expected from bias discrepancy may be introduced. For example, the amplifier may be operating in a non-linear region, or excessive movement of the sensitive element may take the restoring coil into non-linear regions of magnetic field. The manner in which amplifier output current, and sensitive arm deflection, typically vary with frequency for a constant vibration amplitude is illustrated in Figs. 11, 14 and 17. The contrast between air-filled and oil-filled instruments should be noted. When the amplitude of vibration becomes greater still the amplifier will reach saturation (this usually happens first) or the sensitive element will reach its limit stops and the instrument will effectively cease to function. As mentioned in Section 3.3, the effective operating range for steady acceleration is reduced by the peak value of any vibration which is simultaneously present; the reduction can be even greater near the resonant frequency of the loop, as indicated in Fig. 11.

(iii) High frequency vibrations in any direction may set up local resonances in the component parts of the instrument e.g. the pendulum arm might vibrate like a string in various modes. With careful design these effects should not be important.

(iv) When the vibration is applied at such an angle that it has a component both along the sensitive axis and in a plane normal to the sensitive axis various effects which may cause rectification can occur, but since these effects are different for the two types of accelerometer they are discussed separately in Sections 4.2.3 and 4.3.2 below. For the pivoted-arm type the man effect is due to cross-coupling.

Some typical vibration results are given in Fig. 7, for an air-filled accelerometer. From the point of view of performance under steady acceleration conditions it is important to keep to a minimum the displacement of the sensitive element from null. This implies a high loop gain and hence a fairly high resonant frequency with low damping. This characteristic is bad from the point of view of vibration, so there is some conflict between the requirements of steady-state accuracy in a quiet environment and reasonable accuracy in a severe environment. Probably the best combination of properties is achieved with the oil-filled accelerometer as this can be operated with a high loop gain combined with optimum damping (0·7 of critical). There is a further discussion of dynamic response in Section 7 and Appendix C.

Circular and angular vibration may also be present in aircraft or missile structures. The exact effects of such vibrations on the accelerometer are difficult to calculate, although there seems to be no obvious

way in which serious errors can arise from this source, except where pivot and jewel suspension is used since circular vibration can then produce significant friction torques.

(b) *Magnetic interference.*

Provided all normal precautions have been observed in the design of the magnet system these accelerometers are not usually affected to any significant extent by magnetic fields of, say, the same order as the earth's field. But they may be used in installations in which they are near a comparatively powerful magnet, in which case errors may be caused. The effect usually takes the form of a change of scale factor due to the temporary redistribution of the active field in the presence of the disturbing magnet.

A second type of error which has been noted occurs when the pick-off is of the inductive type and this can, under adverse circumstances, be affected by either a uni-directional or an alternating disturbing field. This type of disturbance usually results in a shift of the null position with the consequent errors mentioned in 4.1.1(d).

If magnetic screens are used to shield against these effects then the screens should be well protected against mechanical damage or movement since the screens themselves will have a disturbing effect.

(d) *Mass of sensitive element.*

Since the actuating force of an accelerometer is that necessary to accelerate the sensitive element, then the mass of this must remain constant or changes of scale factor will occur. Equation (A.2) shows that the scale factor is directly proportional to the mass of the sensitive element. The main way in which the mass can change is by the absorption of water vapour into the materials of which the sensitive element is built.

It has been established that a piece of dural sheet anodised to Specification D.T.D. 610c (sulphuric acid) will absorb up to 1 mgm of water per square inch of surface area under conditions of 100 per cent relative humidity. This could cause a total effective mass change of approximately 4 mgm at the pick-off coil in a typical pivoted-arm sensitive-element assembly having an effective mass at the pick-off coil of 3 gm, and would correspond to an increase in scale factor of 13 parts in 10^4. Anodising to the same specification but with chromic acid would reduce this effect to less than 1 part in 10^4.

Similarly, the pick-off and restoring coils will absorb moisture. It is possible to limit this by 'potting' the coils in a suitable compound such as one of the 'araldite' group of non-hygroscopic adhesives.

Individual accelerometers of the same type will have slightly different coefficients of scale-factor variation with relative humidity, and there is the added complication that the effect has a time-lag of some 20–30 hours for an unsealed instrument of typical design.

Another effect which can introduce apparent changes of mass is the buoyancy of the air surrounding the sensitive element. The total effect of this (say, if all the air was removed) is about 3 parts in 10^4, but this does not normally appear as an error since the accelerometers are usually mounted in sealed canisters full of air at ground density. It should be noted that where unsealed accelerometers of very high accuracy are being tested it is necessary to take account of variations of air density at ground level, since changes of apparent mass of a few parts in 10^5 can occur. In an oil-filled instrument the buoyancy of the oil has a very substantial effect and is the main reason why temperature control is necessary if a constant scale factor is to be maintained.

(e) *Variation of gravity.*

By far the most convenient way of testing an accelerometer is to make use of the steady force of gravity, with the accelerometer stationary on a rigid test fixture. When considering accelerometers of high accuracy, however, it must be remembered that there are limits to the accuracy of our knowledge of the absolute value of the acceleration due to gravity. Measurements taken at Potsdam are usually referred to for the absolute value and these figures appear to be reliable to about 1 part in 100 000. The variation with geographical position is considerable, the change being primarily a function of latitude. From the equator to the poles the total change is about 1 part in 200 and in England the rate of change is about 1 part in 10 000 for every 70 miles in the north-south direction. Superimposed on this are local effects due to the particular geological formations in any area. The value of gravity can be calculated for any position at which it is required from the formula

$$g = 978{\cdot}049\,(1 + 5288{\cdot}4 \times 10^{-6} \sin^2 \phi - 5{\cdot}9 \times 10^{-6} \sin^2 2\phi) - 308{\cdot}6 \times 10^{-6} H$$

where g = value of gravity acceleration in cm/sec/sec

ϕ = latitude

H = height in metres.

But it seems that the result derived from this formula should not be regarded as accurate to better than 1 part in 10 000.

Finally, as shown by the equation above, there is a significant change with height amounting to roughly 1 part in 10 000 per 1000 ft of height, (only accurate for small values of H).

Laboratories used for the testing of accelerometers have usually had the local value of g measured by means of a precision gravimeter[8], the figure obtained being repeatable to about one part in 10^6. The method is usually a comparison of the scale reading of a portable gravimeter at the laboratory with that at a reference Gravity Base Station. The g value at the Base Station is already known by a further comparison with a standard Pendulum House.

4.2. *Sources of Error Peculiar to the Pivoted-Arm Type.*

4.2.1. *Shift of centre of mass of sensitive element.* The effects mentioned earlier which can cause a change in the total mass of the sensitive element can also cause a change in the position of the centre of gravity. Also, this type of accelerometer is often provided with cross-balance adjustments specifically for the purpose of adjusting the C of G position. The effect of such a change, after calibration, is primarily to cause a change of scale factor if the shift is along the length of the arm, and to cause a change of axis error if the shift is along the sensitive axis. This is shown by the effect of a change in α in equation (A.1). Linear expansion of the arm due to temperature changes does not usually cause significant changes since the coefficients of expansion of the arm and frame are usually reasonably well matched.

4.2.2. *Shift of zero position of spring hinge.* As mentioned earlier the most accurate accelerometers of the pivoted-arm type make use of a spring hinge pivot rather than jewelled bearings. The reason for this is to avoid uncertainty of friction forces and lack of definition of the point of support. When the mass is supported only by a spring hinge the spring rate must, of necessity, be fairly high. The high spring rate of itself does not introduce errors since it is a linear effect, but it implies that great care must be taken to avoid mechanical or electrical changes which may shift the zero position of the arm. The term $S\rho$ in the numerator of equation (A.1) gives the magnitude of the error since ρ is the total deflection of the spring from its mean position. For the typical values given in Appendix A it is seen that a change of 1′ of arc in ρ will result in the introduction of a bias force equivalent to an error of $17 \times 10^{-4}\,g$.

If the spring hinge has not been sufficiently well aged to relieve any internal stresses due to machining or clamping, then changes greater than this may occur. Such changes may be accelerated by shock or temperature cycles or may appear as a slow drift with time.

4.2.3. *Cross coupling and vibration effects.* When an accelerometer of this type is subjected to an acceleration which does not lie along the sensitive axis, or exactly normal to that axis, then an error is introduced due to the cross-coupling effect as described in Section 3.7 and Appendix A. The error (measured in g's) is given by equation (A.7) as

$$\delta_c \times N \times C.$$

The error is therefore proportional to the cross-coupling coefficient δ_c and to the product of the acceleration components along and across the sensitive axis.

Suppose now that N and C are components of a vibrational acceleration $F \sin \omega t$ acting at angle θ to the sensitive axis, so that

$$N = F \sin \omega t \cos \theta\,, \qquad C = F \sin \omega t \sin \theta\,.$$

For very low frequencies, where the arm deflection may be supposed to be the same as for static conditions, the vibration error due to cross-coupling is

$$\delta_c F^2 \sin^2 \omega t \sin \theta \cos \theta .$$

At higher frequencies we may suppose the arm deflection to be multiplied by a factor q and to lead by a phase angle ϕ compared with its low-frequency response, both q and ϕ being functions of the frequency. Some typical curves of q against frequency are given in Fig. 17. The cross-coupling error is then

$$\tfrac{1}{2} q \delta_c F^2 \sin \omega t \sin (\omega t + \phi) \sin 2\theta .$$

The effect will be a maximum when $\theta = 45°$ and there will then be a steady component of error of

$$\tfrac{1}{4} q \delta_c F^2 \cos \phi .$$

Typically δ_c is 10^{-5} radian/g (2 arc sec/g) and the cross-coupling error at low frequency is then $2{\cdot}5 \times 10^{-6}\, g$ per g^2 of peak vibration. This is usually about an order less than the non-linearity effect (Section 3.6) but it should be remembered that over parts of the frequency spectrum, with an air-filled accelerometer, the magnifying factor q may be as high as 6 or even 10.

4.3. *Effects Peculiar to the Rectilinear Type.*

4.3.1. *Shift of centre of gravity of sensitive element.* One of the advantages of this design is that the calibration is almost entirely independent of the position of the centre of gravity of the sensitive element. This is due to the fact that the displacements which occur are linear rather than angular and all torques are accommodated by changes in tension of individual ligaments, as can be seen in Fig. 20.

4.3.2. *Cross coupling and vibration effects.* The early design of this type of accelerometer used suspension ligaments which were adjusted to have zero tension apart from that introduced by cross acceleration. In this condition a cross coupling error similar to that derived in Sections 3.7 and 4.2.3 for the pivoted arm type, will be present.

To avoid cross-coupling effects the later designs are such that the ligaments are always in tension. When this is done the cross-coupling errors become much less likely to occur, as shown in Appendix A, and no error will arise from purely geometrical considerations due to cross acceleration or vibration. This is only true on the condition that the cross acceleration is not sufficiently large to reduce the tension in any ligament to zero.

A construction using a mass supported by tensional ligaments obviously results in an oscillatory system having very little damping. Used under the normal condition of environmental vibration, resonances leading to ligament fracture would be almost inevitable. The design of the instrument must therefore provide additional damping to give adequate protection against this possibility.

4.3.3. *Shift of null point of pick-off.* As a result of using ligaments in tension the instrument is made more sensitive to any change of the mean operating position of the sensitive element, i.e. to the position of the null point of the pick-off. This can be seen in equation (A.8) of Appendix A in which a change of null position is represented by a change in the value of ρ. The effect may be large since ligaments under tension act in the same manner as a relatively stiff spring and therefore a small change in null position can introduce a large bias force.

A secondary effect of the ligament tension is that movement of the sensitive element must tend to stretch the ligaments and therefore to increase the tension. This effect is proportional to the square of the displacement and if it is of significant magnitude, errors in linearity will result.

5. *Methods of Testing Pivoted Arm Accelerometers in Open-Loop.*

5.1. *Pick-off Sensitivity and Hinge Stiffness.*

The accelerometer and associated amplifier form a closed-loop system and the bulk of testing is carried out in this condition. A few parameters however can more easily be measured on open loop, that is, without the amplifier in circuit. For example a simple test can measure both the pick-off sensitivity (G_p volts/radian) and the hinge stiffness to applied acceleration (S_a g/radian). The stiffness S_a is equal to S/Mg where S is the stiffness measured in dynes/radian and M is the pendulous mass. In this test the accelerometer is mounted on a dividing head with its arm substantially vertical and the free end uppermost ('hinge-down'). The pick-off voltage is then measured for a small tilt to either side of vertical and by subtraction the change of pick-off output with tilt is calculated (say V_1 volts/radian). The test is repeated in the 'hinge-up' position and another value for change of output with tilt is obtained (V_2 volts/radian). Then it is shown in Appendix B and by reference to Fig. 21a that the required parameters are given by:

$$G_p = \frac{2V_1 V_2}{V_1 - V_2} \text{ volts/radian}$$

$$S_a = \frac{S}{Mg} = \frac{V_1 + V_2}{V_1 - V_2} g/\text{radian}.$$

It is necessary to know the value of G_p in order to decide what gain the amplifier should have to achieve a given static deflection of the arm per unit acceleration in closed loop. Knowledge of both G_p and S_a is necessary to calculate the total loop gain and hence to estimate the magnitude of second order effects such as the change of scale factor with amplifier gain.

5.2. *Time-Constant.*

This test is applied to oil-filled accelerometers for the purpose of measuring the viscous properties of the oil in terms of a time-constant. The accelerometer is mounted in the zero-g hinge-up position and the pendulous arm is deflected by passing a current through the restoring coil. The current is removed and the time-constant (τ) of the pick-off voltage as it falls towards zero is measured i.e. the time to fall from V volts to 0·368 V volts. It is shown in Appendix B that the viscous-damping coefficient of the oil (D dynes per cm/sec) is given by

$$D = \frac{(S + Mg)\tau}{r}$$

where r is the radius of the arm from the hinge to the centre of the pendulous mass.

Further discussion of open-loop testing is given in Ref. 9.

6. *Methods of Testing in Closed Loop.*

6.1. *Tests in the Range $+1\,g$ to $-1\,g$.*

As mentioned ealier, by far the most convenient way in which to test an accelerometer is by observing its output when the sensitive axis is positioned at various angles relative to the local gravity vector. Fortunately this method of testing is capable of providing a large amount of information even though the value of the test accelerations, $+1\,g$ to $-1\,g$, may be only a fraction of the range of the instrument under test. A rather undesirable but unavoidable feature of these tests is that for every position except $+1\,g$ and $-1\,g$ there is a cross acceleration present.

The first requirement before such tests can be carried out is to have a goniometer or dividing head which is sufficiently accurate and reliable (about 2 seconds of arc for the types of accelerometer under discussion). This goniometer must, of course, be mounted on a rigid foundation if its accuracy is not to be lost by flexure of its support. A bracket, also very rigid and of non-magnetic material, must be attached

to the goniometer head in such a way that the accelerometer mounting face will be truly vertical when the goniometer reading is 0° or 180° and truly horizontal when the reading is 90° or 270°. It is an advantage if the assembly is such that the accelerometer can be rotated about its nominal sensitive axis when required.

The electrical connections will vary with the particular unit, but it is essential to take all the usual precautions in the measuring circuits consistent with the high order of accuracy required. A schematic diagram and list of components of a typical test layout is given in Fig. 8. A resistor (referred to as the readout resistor) is connected in series with the force coil and the voltage drop across it is taken as the output of the accelerometer. The readout resistor must therefore be a well-aged and stable standard, the value of which is accurately known (a convenient value is that which gives 1 V per g). If possible it should be connected into the earthy end of the circuit to avoid leakage difficulties. A multi-range centre-zero dc ammeter is connected into the restoring circuit in order to check the amplifier unbalance under no-signal conditions. The precautions to be taken with the measuring potentiometer and standard cell are well-known. In addition, a calibrated thermometer reading to 1/10 deg. C is required and a continuous record of the relative humidity in the test area (for unsealed accelerometers). For some purposes it may be found that a digital voltmeter is sufficiently accurate to take the place of the potentiometer/galvanometer measuring circuit. Digital milliammeters are under development which will eliminate the readout resistor as well.

When carrying out a calibration test on this fixture the accelerometer should be switched on for sufficient time to attain stable temperature conditions before accurate readings are attempted. A convenient order in which to take the readings is given in Appendix D which shows a typical test sheet and analysis to give scale factor, bias force, component of axis error and linearity over the range $+1\ g$ to $-1\ g$. The readings taken at 10 minutes of arc on either side of the 0° and 180° settings are not essential, but provide a convenient and simple method of obtaining the bias force and component of axis error with little chance of arithmetical mistakes. This is shown in Fig. 9. It will be noted that a number of readings have been repeated at various stages during the test and the accuracy of these repetitions is a useful indication of the behaviour of the instrument and a check of the test equipment.

To obtain the total axis error, as distinct from the component measured above, it is necessary to set the goniometer to 0° (i.e. mounting face accurately vertical and therefore output approximately zero) and then to take readings as the accelerometer is rotated to various positions around its nominal sensitive axis. A plot of these results (Fig. 10) shows a sinusoidal curve displaced from the horizontal axis by an amount which corresponds to the bias force, and the amplitude of the sine wave represents the total axis error. The position of the peak indicates the orientation around the sensitive axis at which the axis error is maximum.

An adequate assessment of the performance standard of an accelerometer can be derived much more quickly normally within 15 minutes, by a 'five-point' test in which the accelerometer output is measured at $+1\ g$, $0\ g$, $-1\ g$, $0\ g$ and a return to $+1\ g$. These applied forces occur at goniometer readings of 90°, 180°, 270°, 0° and back to 90°, respectively. From these results, as in the more comprehensive method, it is easy to determine the bias forces, scale factor and axis error as defined earlier; the fifth point measurement provides the operator with a check that the test conditions have remained stable during the run.

From some hundreds of five-point tests carried out on a large number of pivoted-arm accelerometers it is known that, irrespective of changes in the individual bias forces, the measured bias discrepancy should remain constant to within two or three parts in 10^5 for each instrument. Under normal storage and handling conditions the measured axis error should also stay constant to within the same order of limits. It is therefore possible to check the consistency of the test methods and equipment by comparing these parameters after each test on individual instruments. A typical test sheet is shown in Appendix D, covering a period of six weeks. The accelerometer was tested four times during this period and the results obtained are considered to be of the standard of accuracy and repeatability necessary if an accurate analysis of other sources of error is to be carried out; these include magnetic interference, changes of temperature and power supply, etc.

Although it is not possible to apply accelerations greater than $1\ g$ in these tests, some information can be obtained concerning the performance at higher acceleration. As has been stated earlier the discrepancy between bias values obtained from the $\pm 1\ g$ and null positions is a guide to the magnitude of linearity

errors at higher acceleration levels. A large bias discrepancy is a sure sign that large linearity errors are present.

In fact tests with a precision centrifuge on 14 instruments of the same type, within the range $-10\,g$ to $+8\,g$, showed that the non-linearity was predominantly quadratic and correlated closely with the value of bias discrepancy calculated from the five point test; the average difference between the quadratic coefficient and bias discrepancy was $1{\cdot}5 \times 10^{-5}$ of 1 g, with a standard deviation about this figure of 1×10^{-5} of 1 g (the actual magnitude of the bias discrepancy was about 6×10^{-5} of 1 g, average).

Some information on higher acceleration performance can be obtained at 1 g by shunting the restoring coil with a resistance of, say, one fifth of the coil resistance. Under these conditions the movement of the sensitive element and all the signal levels in the amplifier will be the same as if an acceleration of five times the actual value had been applied. The demagnetising effect of the coil current, heating effects of the coil and distortion of the sensitive element will not be truly represented.

6.2. *Centrifuge Tests.*

It is possible to carry out direct tests at high accelerations by mounting the accelerometer on a rotating arm, but very precise and therefore expensive equipment is required if worthwhile accuracy is to be achieved. The usual type of centrifuge commonly used for examining the effects of high accelerations on instruments is not suitable for accuracy tests of accelerometers. The points requiring special attention for this purpose are the constancy of speed, flexing of the structure, vibration and the ability to mount the accelerometer at a very accurately known radius. The radius required to calculate the value of the applied acceleration is that from the centre of rotation to the centre of mass of the sensitive element; the latter is not usually known very accurately, and changes its position slightly with applied acceleration. There is, of course, an acceleration gradient across the accelerometer which may be troublesome in some cases.

The problem of maintaining the speed of the centrifuge sufficiently constant is one of some difficulty. If an error contribution of 1 part in 20 000 can be tolerated from speed control imperfections then the angular velocity of the centrifuge must be known to 1 part in 40 000 and must be held constant to this order of accuracy whilst a measurement is taken. If the operating radius is about 2 feet then an angular velocity of about 38 rpm will gave a radial acceleration of 1 g. To maintain the desired accuracy this speed must be constant to 0·00096 rpm, i.e. roughly 21° per hour.

The design and development of such centriguges is a major undertaking and they therefore exist only in the principal centres for the evaluation of inertial guidance components. An example is the British Aircraft Corporation centrifuge at Stevenage which has an operating radius of 2 feet and an acceleration maximum of 15 g (at 150 rpm). Modifications are in progress to increase the maximum to 24 g. The speed is measured with a resolution of 1 microsecond per revolution (1 part in 400 000 at 15 g). Changes in radius arm are continuously monitored, and it is stated that the overall acceleration accuracy is 1 part in 100 000.

6.3. *Long-Stroke Vibrator.*

The long-stroke vibrator[10] is designed to provide a long stroke so that reasonably high acceleration levels can be obtained while keeping the frequency low enough to give useful information on the steady-state performance of the accelerometer. In particular it is used for measuring the non-linearity of the accelerometer output at levels greater than 1 g.

If an accelerometer is subjected to linear displacements varying sinusoidally with time about a fixed point, then it will be subjected to a sinusoidally varying acceleration of peak magnitude depending on the amplitude and frequency of the oscillation of displacement.

Assuming that the accelerometer characteristic, although non-linear, is a smooth curve it can be expressed as a polynomial thus:

$$\text{output} = A + Bf + Cf^2 + Df^3 + \ldots.$$

where A, B, ... are constants and f is the acceleration acting on the instrument.

Suppose now that the accelerometer is mounted on the vibrator with its sensitive axis parallel both to the gravity vector and to the line of the linear displacement, and is vibrated. Although the oscillatory accleration being applied has zero average value, owing to the lack of symmetry of the accelerometer characteristic over the range being explored, the resulting output due to the oscillation will have a small unidirectional component, i.e. the output will depart slightly from the static 1 g value. This change in output can be measured to the same order of accuracy as the 1 g output. The measurement can be repeated with the accelerometer turned upside down and with different amplitudes of sinusiodal acceleration.

If the accelerometer is mounted in the $+1$ g position and the sinusiodal acceleration is $F \sin \omega t$ in 'g' units, then substituting in the polynomial we have:

$$\text{Output} = A + B(1 + F \sin \omega t) + C(1 + F \sin \omega t)^2 + D(1 + F \sin \omega t)^3 + \ldots .$$

$$= A + B + C + D + (BF + 2CF + 3DF \ldots) \sin \omega t + (CF^2 + 3DF^2 \ldots) \sin^2 \omega t + DF^3 \sin^3 \omega t \ldots$$

It will be sufficient to take the polynomial as far as the Df^3 term only.

The average value of the output over any number of complete cycles will then be:

$$A + B + C + D + \tfrac{1}{2} CF^2 + 3/2\, DF^2.$$

Evidently $A + B + C + D$ is the static output for 1 g, so that the remaining terms $\frac{1}{2} CF^2 + 3/2\, DF^2$ represent the change in output due to vibration. When the accelerometer is mounted upside down the corresponding change is $\frac{1}{2} CF^2 - 3/2\, DF^2$. The coefficients C and D can therefore be evaluated.

This method avoids the difficulty of accurate measurement of the applied accelerations since the non-linearity is measured directly against the static 1 g value.

6.4. *Vibration Tests.*

Since it is difficult to ensure that the sensitive axis of the accelerometer is accurately fixed in direction when the unit is mounted on the armature of the vibrator, it is preferable to arrange that all vibration tests are carried out with the sensitive axis vertical. In this position small changes of tilt have negligible effect on the output.

The bracket by which the accelerometer is mounted must be a rigid structure and the centre of mass must be on the vibration axis. In spite of rigorous precautions it is usually found in practice that there are resonances in the mounting assembly which make it difficult to obtain accurate results over one or two narrow bands of frequency.

Vibration should be applied along each of the three major axies in turn. For vibration along the sensitive axis, the major effect will be that due to non-linearity, as in the long-stroke vibrator test of Section 6.3. It is helpful to monitor resonances by inserting an ac milliammeter in series with the restoring coil or to connect an oscilloscope across the readout resistor. Typical frequency responses for vibration along the sensitive axis are shown in Figs. 11 and 14. Fig. 7a shows a graph of AC against frequency of applied vibration for a low frequency loop with poor damping and Fig. 7b shows the acceleration amplitude which makes the accelerometer readings useless, i.e. when the sensitive element touches its limit stops. Fig. 7c shows the effect of minimizing the lack of symmetry mentioned in 4.1.1(b).

Vibration should also be applied at an angle of 45° to the sensitive axis in order to check the cross-coupling effects described in Section 4.2.3. It should be noted that both cross-coupling and non-linearity effects are present in this test.

Particularly in the case of the rectilinear accelerometer, in which the sensitive element is supported by thin ligaments, it is possible that severe vibration will cause mechanical failure of the suspension resulting in gross errors in the output. Since the result of such a failure in service may be disastrous, the vibration tests should be made over a range of amplitudes and frequencies which cover that expected in service with a reasonable safety factor.

6.5. *Servo Loop Stability Tests.*

Since the accelerometer as a whole with its amplifier constitutes a high-gain closed-loop servo system, problems of stability arise. The detail of the methods for carrying out tests to determine the stability margin will depend upon the particular nature and arrangement of the circuits employed, but in any case normal servo analysis techniques are used.

It is usually difficult to carry out simple open-loop tests on an undamped accelerometer (i.e. with the loop broken so that the sensitive element is uncontrolled) since in this condition the accelerometer is extremely sensitive to ground vibrations which are likely to be present at most test sites. Even when the test fixtures is mounted on a solid concerete foundation and well away from running machinery, it will be found that building vibration makes accurate testing difficult.

It is possible however to carry out an open-loop test on an oil-filled accelerometer and its amplifier by disconnecting the output of the amplifier from the restoring coil and feeding the output current instead into an equivalent resistance (or the restoring coil of another accelerometer of the same type so that the circuit impedance remains the same). A known current of variable frequency is then fed into the restoring coil of the first instrument and the open-loop response determined by measuring the amplifier output current.

A closed-loop test may be performed on either a damped or undamped accelerometer by injecting the disturbing signal at any convenient point (e.g. the input of the amplifier dc stage) and observing the response. The usual precautions are necessary to ensure that the signal injection circuit is not affecting the normal operation of the system.

Closed-loop tests may also be performed mechanically by means of a vibrator. It is necessary to monitor the applied vibration by means of another accelerometer of wide frequency response; the restoring coil current of the accelerometer under test is then measured in amplitude and phase relative to the applied vibration. The test demands a vibrator of good waveform and is usually only suitable for the lower frequencies.

The object of these tests is to ensure that the system is sufficiently damped with reasonable phase and gain margins and to show that this condition is maintained for all expected environmental conditions and the effects of changes in the electronic components. The tests are also useful for predicting the transient behaviour of the loop e.g. the response to step or ramp accelerations. A knowledge of the frequency response can also help to predict vibration-included errors e.g. those due to cross-coupling (Section 4.2.3).

7. *Dynamic Response.*

The characteristics of the dynamic response are of interest not only from the point of view of stability but also when rapidly changing accelerations are being measured. An analysis is given in Appendix C. The general shapes of the frequency-response curves (in amplitude/phase and Nichols form) for air-filled and oil-filled pivoted arm accelerometers are shown in Figs. 11, 12, 14 and 15. These curves are plots of the amplitude and phase of the restoring coil current relative to its static or low-frequency value for a constant amplitude of applied acceleration. Both air-filled and oil-filled accelerometers give rise to systems which are approximately of the second order, that is they are described by a natural frequency and a damping coefficient, but whereas with an oil-filled instrument it is fairly easy to achieve the desirable damping coefficient of about 0·7 of critical, with an air-filled instrument it is difficult to achieve damping better than about 0·3 of critical. In fact the curves of Figs. 11 and 12 indicate a damping coefficient of about 0·18 and this could be improved by redesign of the response shaping network.

Since the figures mentioned above show very considerable changes of scale factor (mA/g) with frequency, it is seen that if an accelerometer is used for measuring vibration rather than steady acceleration it can obviously do so accurately only at frequencies well below the natural frequency. Fig. 18 plots the fractional error due to the dynamic response at various values of the ratio of vibration frequency to natural frequency. If the frequency response of the loop has previously been measured (Section 6.5) it is possible to allow for its effect, but no great accuracy can be achieved (compared with the static accuracy) because various factors such as change of amplifier gain or excitation level have a much greater effect on the dynamic response than on the static accuracy.

Sometimes the response to a step or a ramp acceleration is important. For a natural frequency of 400 c/s and 0·3 damping the response to a step acceleration is oscillatory, the time-constant of the envelope being 1·3 *mS* so that the settling time is about 4 *mS*. For 0·7 damping these figures are approximately halved. The response to a ramp acceleration is a ramp lagging by 0·24 *mS* for 0·3 damping and about twice this value for 0·7 damping.

8. *Conclusions.*

8.1. *Testing.*

When accelerometers of the order of accuracy described in this Report (about 1 in 10^4) are tested, all possible precautions associated with precision measuring techniques must be taken. Also each test should be devised so that repeat readings of the most significant measurements are obtained as the test proceeds.

Testing for performance at accelerations greater than 1 g presents some difficulty, but much information can be obtained by shunting the restoring coil and by vibration tests including the use of a long-stroke vibrator. The most direct method of measurement is by means of a precision centrifuge when this expensive equipment is available.

Accelerometers of the types described are instruments of extremely high precision by any normal standards, being sensitive to a change of acceleration which is not much more than one millionth of their maximum reading. Hence where instruments of this type must be used they should be handled carefully and stored in reasonable conditions; also the most advantageous environment possible should be provided for them when they are in service use. Very careful attention must be paid to the environment in which any accuracy tests are carried out.

8.2. *Performance.*

Typically, precision accelerometers may be used to measure acceleration within the range $\pm 15\,g$, which may be extended to $\pm 20\,g$ for short periods and with suitable design of the electronics. Accuracy may be as good as 0·01 per cent provided that the various performance parameters have been accurately predetermined and that it is possible to make full allowance for those known errors. This situation rarely applies in practice and a rough figure of 0·03 per cent of the acceleration or $6 \times 10^{-4}\,g$, whichever is the greater, is the order of accuracy to be expected in typical system environments with calibration at three monthly intervals. At low acceleration the bias (about $4 \times 10^{-4}\,g$) is the most significant component of error and at high acceleration the quadratic error (about $0{\cdot}5 \times 10^{-4}\,g$ per g^2) usually predominates.

The main application of the instruments is in inertial navigation where their output is integrated to obtain vehicle velocity. The emphasis in design has therefore been on static or low-frequency accuracy. However, their response times are low enough (a few milliseconds) to follow fairly rapid changes of acceleration, and they may also be employed to measure vibration provided the frequency is well below the natural frequency of about 400 c/s.

REFERENCES

No.	*Author(s)*	*Title, etc.*
1	I. L. Thomas, R. W. Plumbly and R. J. Pitt	Sources of error in precision force-feedback accelerometers, and methods of testing. R.A.E. Technical Note IAP 1076 (1960).
2	R. H. Evans and G. G. Haigh	Feedback accelerometer circuits with a velocity output. Aeronautical Research Council R. & M. 3462 (1964).
3	R. J. Pitt and M. Crosby	Performance details of single axis accelerometers Mark I. R.A.E. Technical Note IAP 1124 (1960).
4	R. W. Plumbly, R. J. Pitt and R. H. Evans	An assessment of a precision, viscous-damped force-feedback accelerometer. R.A.E. Technical Note IAP 1135 (1961).
5	R. W. Plumbly, M. G. Howson and Miss D. Shearing	A further assessment of a precision viscous-damped force-feedback accelerometer. R.A.E. Technical Note IEE 3 (1962).
6	J. Appleton	An analysis of an eddy current pick-off. R.A.E. Technical Report 66270 (1966).
7	J. M. Cockcroft	Methods of linear temperature compensation of the scale factor of a force-feedback accelerometer. Ferranti Report AELB/76 (1963).
8	J. M. Spatcher	Some precise measurements of the acceleration due to gravity. R.A.E. Technical Memo IEE 151 (1966).
9	J. M. Cockcroft	Theory of the method of open-loop testing of force-feedback accelerometers. Ferranti Aircraft Equipment Laboratory. Report No. 74 (1965).
10	J. Davies	The long stroke vibrator. Ferranti Aircraft Equipment Laboratory. Report No. 22 (1962).

APPENDIX A

Static Operating Conditions.

A.1. *Symbols.*

Many of the parameters are illustrated in Figs. 19 and 20.

M	Mass of sensitive element (gm)
T	Tension in suspending member (dynes)
I	Force coil current (amp)
K_c	Force per unit current in force coil (dynes/amp)
G	Pick-off and amplifier gain (output current per unit angular deflection of the suspending member) (amp/radian)
S	Spring rate of all spring-like forces combined (dynes/radian)
I_u	Amplifier unbalance (output current for zero input) (amp)
g	Acceleration due to gravity (cm/sec^2)
Ng	Acceleration along sensitive axis (normal to mountain face) (cm/sec^2)
Cg	Acceleration normal to sensitive axis (cm/sec^2)
b	Constant force acting in one direction along sensitive axis (dynes)
n	Total number of suspension ligaments
ρ	Angle through which the effective spring is deflected from its free position when the pick-off is at null (radian)
λ	Angle between ligaments and their clamping plane when no other forces are acting (radian)
α	Angle between line joining pivot to the cg and the plane of the mounting face when the pick-off is at null (radian)
β	Angle moved through by pick-off to produce signal necessary to counteract effect of I_u (radian)
γ	Corresponding angle as above to counteract bias force b (radian)
δ	Corresponding angle as above to counteract acceleration forces (radian)
ε	Angle between sensitive axis and line of action of force coil (radian)
δ_c	Cross coupling coefficient, equal to the angle moved through by the arm per g of acceleration along the sensitive axis (radian/g).

A.2. *Sources of Error.*

The major source of error of acceleration of both the pivoted arm and parallel motion types of accelerometer are indicated by the force balance equations derived below for steady state conditions. In the case of the pivoted arm type it has been possible to include in the equations nearly all the possible misalignments which can lead to errors of the output. Unfortunately this would be much more difficult in the case of the rectilinear type and the discussion has been restricted to an accelerometer with tensioned ligaments, all the tension being equal in the absence of any other forces, and with perfectly symmetrical geometry of the suspension, central mass and outer frame. Various forms of lack of symmetry and unequal tensions may give rise to errors of all types, particularly when such defects occur in combination with the usual bias forces and axis errors. It is not intended to discuss these effects in this Report.

A.3. *Pivoted-Arm Type.*

The mode of operation and the forces concerned in a pivoted-arm type accelerometer are shown in Fig. 19. The arm is pivoted at A and AA' is a line parallel to the mounting face and normal to the hinge axis. The pick-off is shown diagrammatically as a potentiometer, the wiper of which is connected to an amplifier of gain G; the accelerometer force coil being in the output circuit of the amplifier. The position of the arm is represented by the line joining the hinge centre to the cg of the arm.

The positions 1, 2, 3, 4 along the potentiometer represent:

(1) Is the arm position for which the pick-off output is zero. This therefore represents the position which the arm will take when there are no forces of any sort and no unbalance in the amplifier.

(2) Is the arm position when no bias or acceleration forces are present, but the amplifier is unbalanced to produce an output current I_u for zero input.

(3) Is the arm position when both unbalance and bias force are in action but no accelerations are applied.

(4) Is the final working position when accelerations Ng and Cg are applied together, Ng being normal to the mounting face and Cg at right angles to Ng in the plane of the arm.

The gain (G) of the amplifier is expressed as the output current per unit angular movement of the arm, and the force coil constant K_c represents the force on the arm per unit current. To avoid confusion due to the various radii all forces are assumed to act at the centre of mass of the arm.

From the force diagram of Fig. 19 we have

$$K_c I \cos(\varepsilon+\alpha+\beta+\gamma+\delta)+S(\rho+\beta+\gamma+\delta)+M\,Cg \sin(\alpha+\beta+\gamma+\delta) = b+MNg\cos(\alpha+\beta+\gamma+\delta)$$

and assuming all the angles are small we have

$$K_c I+S(\rho+\beta+\gamma+\delta)+MCg(\alpha+\beta+\gamma+\delta) = MNg+b\,.$$

But

$$I = G(\beta+\gamma+\delta)+I_u$$

or

$$(\beta+\gamma+\delta) = \frac{I}{G}-\frac{I_u}{G}.$$

Substituting for this in above gives

$$K_c I+S_\rho+\frac{SI}{G}-\frac{SI_u}{G}+MCg\,\alpha+\frac{MCg\,I}{G}-\frac{MCg\,I_u}{G} = MNg+b$$

$$I\left(K_c+\frac{S}{G}+\frac{MCg}{G}\right) = -S_\rho+\frac{SI_u}{G}-MCg\,\alpha+\frac{MCg\,I_u}{G}+MNg+b$$

therefore

$$I = \frac{MNg+b-MCg\left(\alpha-\dfrac{I_u}{G}\right)-S\left(\rho-\dfrac{I_u}{G}\right)}{K_c+\dfrac{S}{G}+\dfrac{MCg}{G}}. \qquad \text{(A.1)}$$

Hence in the absence of all the unwanted terms b, C, α, ρ and I_u we have

$$I = \frac{MNg}{K_c + \frac{S}{G}}$$

or

$$\text{Scale factor (amp/g)} = \frac{Mg}{K_c + \frac{S}{G}} \tag{A.2}$$

i.e. the scale factor is dependent mainly on the mass of the sensitive element and the force/current characteristic of the coil and magnet. The term S/G in the denominator is normally small, but implies that there will be small changes of scale factor with changes of amplifier gain.

When no accelerations are present

$$I_b \simeq \frac{1}{K_c}\left\{b - S\left(\rho - \frac{I_u}{G}\right)\right\} . \tag{A.3}$$

which gives the current output normally referred to as the *bias force at zero g*. The predominant term here is normally $S\rho$, and since ρ is a measure of the relative positions of the pick-off null and the zero-force position of the spring, then changes in either of these would give rise to a change of bias force.

When only cross acceleration is present and bias force is zero we have

$$I \simeq \frac{1}{K_c}\left\{MCg\left(\alpha - \frac{I_u}{G}\right)\right\} . \tag{A.4}$$

In this case I_u/G is comparatively negligible and the error term is proportional to α. This angle is the one referred to as the axis error, or more correctly as the component of axis error in the plane of the arm.

To give numerical values for a typical instrument

$$\begin{aligned} K_c &= 0{\cdot}2 \text{ Mg dynes per mA (i.e. 5 mA/g)} \\ G &= 5 \times 10^5 \text{ mA per rad} \\ S &= 6 \text{ Mg dynes per rad} \\ I_u &< 1 \text{ mA} \\ b &< 10^{-4} \text{ Mg dynes} \\ \alpha &< 20 \text{ seconds of arc} \\ \rho &< 10 \text{ seconds of arc.} \end{aligned}$$

Hence the value of I_u/G is seen to be less than 0·5 seconds of arc and is therefore negligible.

Also the term S/G in equation (A.2) has the value $10^{-5}\,Mg$ and is therefore only one twenty thousandth of the value of K_c. Hence the scale factor will change by 1 part in 20 000 if the gain decreases by a factor of two. The term $K_c\,G/S$ is the open-loop gain of the system, in this case equal to 20 000.

Finally the term MCg/G appearing in the denominator of equation (A.1) shows that even when the axis error is zero there will be an error due to the cross acceleration. This is referred to as the *cross coupling effect* and is obviously reduced by making G as large as possible. Ignoring the other small terms in equation (A.1) we have:

$$I = \frac{MNg}{K_c + \frac{MCg}{G}}$$

$$= \frac{MNg}{K_c}\left[1 + \frac{MCg}{K_cG}\right]^{-1}$$

and since $MCg << K_cG$ this expands to

$$I = \frac{MNg}{K_c}\left[1 - \frac{MCg}{K_cG}\right].$$

The first term in this expression is the output expected from the acceleration N and the second term is the error due to the cross acceleration C. Denoting this cross coupling error current I_{cc} we have

$$I_{cc} = \frac{MNg}{K_c} \times \frac{MCg}{K_cG} \tag{A.5}$$

or if we write δ_c in place of Mg/K_cG then

$$I_{cc} = \delta_c \times \frac{Mg}{K_c} \times N \times C \tag{A.6}$$

and

$$\frac{I_{cc}}{I_{1g}} = \delta_c \times N \times C. \tag{A.7}$$

The term δ_c (which represents the angle moved through by the arm per g of acceleration along the sensitive axis) is known as the *cross-coupling coefficient*. The way in which this term gives rise to rectification under vibration is covered in 4.2.3 in the body of this paper.

A.4. *Rectilinear Type.*

Fig. 20 illustrates the action of the forces in the case of the rectilinear type of accelerometer. For the sake of simplicity it has been assumed that the ligaments have equal tensions which change only in the presence of cross acceleration, and that the central arm is slightly longer than the cylindrical frame. Hence with no accelerations applied and with the feedback disconnected the arm will take up a central position with the ligaments inclined at an angle λ at each end. Now if the feedback loop is closed but no acceleration, unbalance current or bias are present, the position detector will move to position (1) i.e. very near to the null point of the potentiometer. This will result in the ligaments becoming inclined at $\lambda+\rho$ on one side and $\lambda-\rho$ on the other.

Now if unbalance current is introduced the wiper moves through angle β to position (2); then bias force b moves the wiper through angle γ to position (3) and finally the accleration forces move it through angle δ to position (4). The pick-off is actually one which is sensitive to linear motion but it is more convenient to treat the displacements as angles moved through by the supporting ligaments, these angles being small.

It should be noted that b is a constant force from any arbitrary source and that T (assumed to be constant) acts as a spring rate such that the total restoring force in position (4) will be $nT\ (\rho+\beta+\gamma+\delta)$ where n is the total number of ligaments. It can be shown that this is a close approximation to the truth even in the presence of cross acceleration, *provided no ligament becomes slack.*

From the diagram in Fig. 20 we have

$$K_c I + nT(\rho+\beta+\gamma+\delta) + MCg\alpha = MNg + b$$

but

$$I = G(\beta+\gamma+\delta) + I_u$$

therefore

$$(\beta+\gamma+\delta) = \frac{I}{G} - \frac{I_u}{G}$$

therefore

$$K_c I + nT\rho + \frac{nT I}{G} - \frac{nT I_u}{G} + MCg\alpha = MNg + b$$

$$I = \frac{MNg + b - MCg\alpha - nT\left(\rho - \frac{I_u}{G}\right)}{K_c + \frac{nT}{G}}. \tag{A.8}$$

Hence in the absence of all the unwanted terms, b, C, α, ρ and I_u we have

$$I = \frac{MNg}{K_c + \frac{nT}{G}}$$

or

$$\text{Scale factor (amp/g)} = \frac{Mg}{K_c + \frac{nT}{G}}. \tag{A.9}$$

Hence as before the scale factor depends on the mass and the coil and magnet assembly characteristic with a small term determined by ligament tension. Again the small term will vary with amplifier gain.

The analysis of the equation to show the appearance of bias force and axis error is identical with that given earlier for the pivoted arm accelerometer.

One significant feature which will be noted is that there is now no term dependent on C in the denominator and hence cross coupling does not occur with this type of suspension. This is only true because of the simplifying assumptions made with regard to constancy and equality of ligament tensions and the general symmetry of the assembly. Since combinations of discrepancies can be envisaged for which the ligament tension becomes a function of acceleration, then small linearity errors and cross coupling effects can occur, but such a detailed analysis is outside the scope of this Report.

APPENDIX B

Analysis of Open-Loop Tests (Pivoted Arm Type Accelerometer)

B.1. *Symbols* (*see* Fig. 21).

G_p	Pick-off sensitivity (volts/radian)
S	Spring rate in terms of linear force (dynes/radian)
S_a	Spring rate in terms of acceleration (g/radian)
M	Mass of sensitive element (gm)
g	Acceleration due to gravity (cm/sec^2)
r	Radius of arm from hinge to centre of pendulous mass
D	Viscous damping coefficient (dynes per cm/sec)
τ	Open-loop time-constant of arm
V_1	Change of pick-off output with tilt (hinge down) (volts/radian)
V_2	Change of pick-off output with tilt (hinge up) (volts/radian).

B.2. *Pick-Off Sensitivity and Hinge Stiffness.*

The test is described in Section 5.1. Referring to Fig. 21a we have that if the accelerometer frame is tilted by an angle θ from the null position, then in the 'hinge-down' position the arm will tilt a little more than θ, and in the 'hinge-up' position will tilt a little less, owing to the action of gravity.

For the hinge-down position, the pick-off voltage will be $V_1\,\theta$ and the deflection of the arm relative to the frame is therefore $V_1\,\theta/G_p$ radian. The total angle that the arm makes with the vertical is therefore $\theta+V_1\,\theta/G_p$. The component of gravity perpendicular to the arm (expressed as a fraction of g) is therefore $\theta+V_1\,\theta/G_p$. But since the arm deflection is $V_1\,\theta/G_p$ the spring force balancing gravity is $S_a\,V_1\,\theta/G_p$. Hence

$$\theta+\frac{V_1\,\theta}{G_p}=\frac{S_a\,V_1\,\theta}{G_p}$$

or

$$G_p+V_1=S_a\,V_1\,. \tag{B.1}$$

Similarly, for the hinge-up position the angle the arm makes with the vertical is $\theta-V_2\,\theta/G_p$ and we have

$$\theta-\frac{V_2\,\theta}{G_p}=\frac{S_a\,V_2\,\theta}{G_p}$$

or

$$G_p-V_2=S_a\,V_2\,. \tag{B.2}$$

By subtraction of equations (B.1) and (B.2) we obtain

$$S_a=\frac{V_1+V_2}{V_1-V_2} \tag{B.3}$$

and by division of equations (B.1) and (B.2) we obtain

$$G_p = \frac{2V_1 V_2}{V_1 - V_2}. \tag{B.4}$$

B.3. *Viscous Damping.*

In the experiment to measure the time-constant τ of an oil-filled instrument (Section 5.2) the relationship between τ and D may be deduced as follows. Reference is made to Fig. 21b.

When the angular deflection of the arm is θ, the total forces tending to restore it to the null position are $Mg\,\theta$ due to gravity and $S\,\theta$ due to the hinge stiffness. The viscous force resisting the motion is $D\,r\,\dot{\theta}$ and the equation of motion is therefore

$$D\,r\,\dot{\theta} + (S + Mg)\,\theta = 0.$$

This equation has the solution

$$\theta = \theta_0\, e^{-t/\tau}$$

where θ_0 is the original deflection and

$$\tau = \frac{Dr}{S + Mg}.$$

Hence if we measure τ, we may calculate D from

$$D = \frac{(S + Mg)\,\tau}{r} = \frac{(S_a + 1)\,Mg\,\tau}{r}. \tag{B.5}$$

APPENDIX C

Analysis of Dynamic Performance.

C.1. *Symbols* (*see* Fig. 22).

x_i	Linear displacement of accelerometer frame (cm)
x_0	Linear displacement of sensitive element (cm)
d	Pick-off displacement (cm)
r	Radius of arm from hinge to centre of mass (cm)
M	Mass of sensitive element (gm)
g	Acceleration due to gravity (cm/sec^2)
S_1	Linear spring rate measured in terms of force (dyne/cm)
S_a	Angular spring rate measured in terms of acceleration (g/radian)
K_c	Force of sensitive element per unit force coil current (dynes/amp)
I	Force-coil current (amp)
D	Viscous damping coefficient (dynes per am/sec)
G_1	Force-coil current per unit deflection of pick-off (amp/cm)
δ_c	Angle moved through by the arm per g of acceleration along the sensitive axis (radian)
τ	Open-loop time-constant of arm (viscous damped accelerometer) (seconds)

C.2. *General Equations.*

Referring to Fig. 22 we have

$$M\ddot{x}_0 = S_1 d + K_c I + D\dot{d}.$$

But

$$d = x_i - x_0 \text{ and } \ddot{x}_0 = \ddot{x}_i - \ddot{d}$$

therefore

$$M\ddot{x}_i = S_1 d + K_c I + D\dot{d} + M\ddot{d}.$$

Now assuming linear performance of all components

$$I = G_1 d$$

therefore

$$M\ddot{x}_1 = \frac{M}{G_1}\ddot{I} + \frac{D}{G_1}\dot{I} + \left(\frac{S_1}{G_1} + K_c\right) I$$

therefore

$$\ddot{x}_1 = \left\{ \frac{M}{K_c G_1} p^2 + \frac{D}{K_c G_1} p + \frac{S_1}{K_c G_1} + 1 \right\} \left(\frac{K_c I}{M} \right).$$

where p is the differential operator.
The quantity $K_c I/M$ is a method of expressing the output current of the accelerometer in terms equivalent to an acceleration ($= \ddot{x}_0$)

therefore

$$\frac{\ddot{x}_0}{\ddot{x}_i} = \frac{\dfrac{K_c G_1}{M}}{p^2 + \dfrac{D}{M} p + \dfrac{S_1 + K_c G_1}{M}}. \tag{C.1}$$

This is the *closed-loop* dynamic-response equation and shows that the undamped natural frequency of the closed-loop system is given by

$$\omega_c = \sqrt{\frac{S_1 + K_c G_1}{M}}$$

and since $S_1 << K_c G_1$

$$\omega_c \simeq \sqrt{\frac{K_c G_1}{M}}. \tag{C.2}$$

In the steady state

$$\frac{\ddot{x}_0}{\ddot{x}_i} = \frac{K_c G_1}{S_1 + K_c G_1} \simeq 1.$$

The open-loop characteristic is given by

$$\frac{\ddot{x}_0}{\ddot{x}_i} = \frac{\dfrac{K_c G_1}{M}}{p^2 + \dfrac{D}{M} p + \dfrac{S_1}{M}} \tag{C.3}$$

in which case the undamped natural frequency is very low

$$\omega_0 = \sqrt{\frac{S_1}{M}}, \tag{C.4}$$

and the steady state condition is given by

$$\frac{\ddot{x}_c}{\ddot{x}_i} = \frac{K_c G_1}{S_1},$$

which is the ratio of the electrical spring rate to the mechanical spring rate.

It may be of interest to note that $K_c G_1/S_1$ is also the total loop gain, that is, the product of all gains around the loop. Also, the ratio of closed-loop natural frequency to open-loop natural frequency is given by

$$\frac{\omega_c}{\omega_0} = \sqrt{\frac{K_c G_1}{M}\frac{M}{S_1}} = \sqrt{\frac{K_c G_1}{S_1}}$$

$$= \sqrt{\text{LOOP GAIN}}$$

As mentioned in Appendix A an important parameter to be controlled in the pivoted-arm type accelerometer is the static angular deflection per g of acceleration (δ_c radian/g) since this determines the sensitivity to cross acceleration. We may write the closed-loop natural frequency in terms of δ_c by substituting

$$\delta_c = \frac{Mg}{K_c G_1 r}$$

and hence obtaining

$$\omega_c = \sqrt{\frac{g}{\delta_c r}}. \tag{C.5}$$

Thus for a given sensitivity to cross-acceleration and a given arm radius, the closed-loop natural frequency is determined. The open-loop frequency of the pivoted arm accelerometer can similarly be written in terms of r and S_a:

$$\omega_0 = \sqrt{\frac{S_a g}{r}}. \tag{C.6}$$

Finally the loop gain has a very simple expression in terms of δ_c and S_a, namely

$$\text{LOOP GAIN} = \frac{1}{\delta_c S_a} \tag{C.7}$$

C.3. *Air-Filled Accelerometer.*

Returning to the transfer function of the closed loop given by equation (C.1) and assuming the viscous damping (D) for air to be negligible, we have:

$$\frac{\ddot{x}_0}{\ddot{x}_i} = \frac{1}{\frac{M}{K_c G_1} p^2 + 1}. \tag{C.8}$$

This represents an undamped oscillatory response to a step change of input, the frequency being ω_c. Since such a response is obviously unsatisfactory it is necessary to add damping electrically, usually by including a phase-advance circuit in the dc stage of the amplifier as shown in Fig. 2. For a pivoted arm accelerometer with typical values of parameters (e.g. $r = 3$ cm, $\delta_c = 1$ arc sec/g $= 0{\cdot}5 \times 10^{-5}$ radian/g) the basic-loop frequency is about 1300 c/s and because it is difficult to stabilise a loop with such a high frequency a lag

circuit is usually incorporated in the amplifier which reduces the gain for all frequencies above say 20 c/s. If the ultimate attenuation of the lag circuit is 9 times, the natural frequency is divided by 3 that is, it becomes 430 c/s, which is a reasonable figure. Fig. 13 shows the frequency response of an amplifier designed for an air-filled accelerometer. The output amplitude is given in terms of *db* relative to its static or low-frequency output for a constant input amplitude. At fairly low frequencies there is a phase lag accompanied by a fall in gain, reaching a trough of 10 *db* down at 130 c/s, and this is followed by a phase lead and rising gain at the phase-advance network takes effect. The corresponding closed-loop response (i.e. restoring coil current for constant amplitude of acceleration) is shown in Figs. 11 and 12. The corresponding deflection of the arm may be obtained by subtracting (in terms of *db* and phase angle) the amplifier response from the current response; applying this procedure to Figs. 11 and 13 produces the curve of Fig. 17.

The lag circuit has the undesirable effect of increasing the arm movement due to low-frequency vibrations (even if the closed-loop response is flat at these frequencies). Another effect is that since the accelerometer itself has a phase lag of 180 deg. at any frequency above its open-loop frequency ω_0 (a few cycles per second), the total phase lag of the loop exceeds 180 deg. at quite low frequencies; hence the loop is conditionally stable, as illustrated by the Nichols chart of Fig. 12. Either a fall in gain of 18 *db* or a rise of 9 *db* would cause the system to become unstable, the oscillation frequencies being 130 c/s and 930 c/s respectively.

From the point of view of the amplitude of the closed-loop response the system is approximately of the second order. The curves shown refer to an inadequately damped loop; more typically the damping coefficient is 0·3 of critical, giving a magnification at resonance of about 1·8 times.

C.4. *Oil-Filled Accelerometer.*

For an oil-filled instrument the damping term D is large and no frequency response shaping circuits are required in the amplifier. For low frequencies, the p term in the denominator of the transfer function predominates over the p^2 term, so that equation (C.1) becomes approximately

$$\frac{\ddot{x}_0}{\ddot{x}_c} = \frac{1}{\frac{D}{K_c G_1} p + 1}. \tag{C.9}$$

This represents a single time-constant response, the time-constant having value $D/K_c G_1$. The bandwidth (i.e. the frequency where the phase lag is 45 deg. and the amplitude is 3 *db* down) is given by

$$\omega_b = \frac{K_c G_1}{D}$$

This may be written

$$\omega_b = \frac{1}{\delta_c (S_a + 1) \tau}$$

for a pivoted arm accelerometer, where S_a is the hinge stiffness in g/radian and τ is the open-loop time constant measured as in Section 5.2. For typical values of the parameters ($\delta_c = 1$ arc sec/g, $S_a = 4$ g/rad, $\tau = 20$ sec) the closed-loop time constant is 0·5 millisecond and the corner frequency ω_b is 320 c/s. The effect of the p^2 term and of other circuit lags usually produces an approximately second order response in which damping is about 0·7 of critical (i.e. there is no resonant peak in the frequency response) and the bandwidth is about 300 c/s.

Figs. 14 and 15 illustrate a typical closed-loop response and Fig. 16 shows that of a typical amplifier. The movement of the arm is shown in Fig. 17. It may be noted that there is no shaping circuit in the amplifier, the response of Fig. 16 being due solely to the smoothing circuit for ripple following the de-

modulator. Neither the current (Fig. 14) nor the arm deflection (Fig. 17) have a resonant peak, and the system therefore has good vibration characteristics. Fig. 15 indicates that the loop will only become unstable for a *rise* in gain (a rise of 12 *db* will cause oscillations at 620 c/s).

C.5. *Additional Comments.*

In practice there are further time lags not fully dealt with in the above analysis. Examples are the smoothing circuit following the demodulator and the inductance of the restoring coil. These effects can be minimised by the use of relatively high frequency for the excitation of the pick-off (e.g. 20 kc/s) and by designing the amplifier to have a high output impedance. There is also a subsidiary feed-back loop due to electromagnetic coupling between the restoring coil and the pick-off, not involving any movement of the suspended element. This coupling can cause troublesome high frequency oscillations, particularly at half the excitation frequency, and these in turn can drive the amplifier into a non-linear region where a low frequency oscillation is triggered off. Thus the choice of stabilising networks is often a compromise between the demands of the various possible modes of oscillation.

Appendix D

Typical Test Results in the Range ±1 g.

Goniometer setting (θ)	Output volts (potentio-meter)	Output corrected for bias	Corrected output scaled to unity max^m for mean of ±1 g	Acceleration applied $\sin(\theta-\phi)$	Error parts in 10^4 of 1 g
359°50′	−0·00014	−0·00344	−0·00312	−0·00313	+0·1
0°00′	+0·00309	−0·00021	−0·00019	−0·00022	+0·3
0°10′	+0·00629	+0·00299	+0·00271	+0·00269	+0·2
15°	+0·2884	+0·2851	+0·25859	+0·25861	−0·2
30°	+0·5543	+0·5510	+0·49977	+0·49981	−0·4
45°	+0·7827	+0·7794	+0·70694	+0·70695	−0·1
(+1 g) 90°	+1·1057	+1·1024	+0·99991	+1·00000	−0·9
135°	+0·7829	+0·7796	+0·70712	+0·70727	−1·5
150°	+0·5546	+0·5513	+0·50005	+0·50019	−1·4
165°	+0·2888	+0·2855	+0·25896	+0·25903	−0·7
179°50′	+0·00671	+0·00341	+0·00309	+0·00313	−0·4
180°00′	+0·00351	+0·00021	+0·00019	+0·00022	−0·3
180°10′	+0·00031	−0·00299	−0·00271	−0·00269	−0·2
0°00′	+0·00305	−0·00025	−0·00023	−0·00022	−0·1
195°	−0·2819	−0·2852	−0·25862	−0·25861	−0·1
210°	−0·5478	−0·5511	−0·49986	−0·49981	−0·5
225°	−0·7763	−0·7796	−0·70712	−0·70695	−1·7
(−1 g) 270°	−1·0993	−1·1026	−1·00009	−1·00000	−0·9
(+1 g) 90°	+1·1057	+1·1024	+0·99991	+1·00000	−0·9
315°	−0·7765	−0·7798	−0·70730	−0·70727	−0·3
330°	−0·5482	−0·5515	−0·50023	−0·50019	−0·4
345°	−0·2823	−0·2856	−0·25905	−0·25903	−0·2
0°00′	+0·00306	−0·00024	−0·00022	−0·00022	0
180°00′	+0·00350	+0·00020	+0·00018	+0·00022	−0·4

N.B. In the above Table the values of bias and axis error used are mean values taken from all the null point observations. Hence some residual error remains at individual null points.

Ambient temperature during test = 21·2°C.

Derivation of Performance Parameters.

Scale factor:

As defined in 3.4 $= \dfrac{I_{+1\,g} - I_{-1\,g}}{2} = K_0$

$$= \frac{1{\cdot}1025 \text{ volts}}{200 \text{ ohms}} \text{ per } g = \frac{5{\cdot}5125\ mA/g}{\text{(Farnborough, Hants.)}}$$

Bias force:

As defined in 3.5 $= \dfrac{I_0 + I_{180}}{2} = B_1$

$$= \frac{0{\cdot}0033 \text{ volts}}{200 \text{ ohms}} = 16{\cdot}5\ \mu A\,.$$

This is normally expressed as a null bias of $+33$ *parts in* 10^4 of 1 g (this would be regarded as an abnormally large error).

Also:

$$= \frac{I_{+1\,g} + I_{-1\,g}}{2} = B_2$$

$$= \frac{0{\cdot}0032 \text{ volts}}{200 \text{ ohms}} = \quad 16{\cdot}0\ \mu A \text{ or } +32 \textit{ parts in } 10^4 \textit{ of } 1\ g \text{ bias.}$$

Bias discrepancy:

$$= B_2 - B_1$$

$$= -0{\cdot}5\ \mu A = -1 \textit{ part in } 10^4 \textit{ of } 1\ g.$$

Axis error:

As defined in 3.2

$$= \frac{I_{180} - I_0}{2} = \alpha$$

$$= \frac{+0{\cdot}00022 \text{ volts}}{200 \text{ ohms}} = +1{\cdot}10\ \mu A = +2{\cdot}2 \textit{ parts in } 10^4\ g.$$

and since 1 part in $10^4\ g = 20$ seconds of arc approx.

$$\alpha = +44 \text{ seconds of arc,}$$

or from the graph on Fig. 9:

$$\text{Bias force} = +0{\cdot}0033 \text{ volts (null readings)}$$

$$\text{Axis error} = +0{\cdot}8' = +48 \text{ seconds of arc.}$$

Single Axis Accelerometer.
'5-point' Test sheet.

Run. No.	*4th August*	*Temperature* 24·9°C	*Relative humidity* 52%
1	Applied g	Output (volts)	Parameters (parts in 10^4 of 1 g)
	+1 g	+1·00131	$B_1 = +1·1$
	0 (hinge up)	+0·00012	$B_2 = +0·8$
	−1 g	−1·00115	$B_2 - B_1 = -0·3$
	0 (hinge down)	+0·00010	Scale factor = 1·00123
	+1 g	+1·00131	Axis error = +0·1
2	*11th August*	*Temperature* 24·5°C	*Relative humidity* 65%
	Applied g	Output (volts)	Parameters (parts in 10^4 of 1 g)
	+1 g	+1·00139	$B_1 = +1·3$
	0	+0·00016	$B_2 = +1·1$
	−1 g	−1·00118	$B_2 - B_1 = -0·2$
	0	+0·00009	Scale factor = 1·00129
	Axis error +1 g	+1·00139	Axis error = +0·35
3	*28th August*	*Temperature* 25·0°C	*Relative humidity* 51%
	+1 g	+1·00136	$B_1 = +0·9$
	0	+0·00012	$B_2 = +0·7$
	−1 g	−1·00122	$B_2 - B_1 = -0·2$
	0	+0·00006	Scale factor = 1·00129
	+1 g	+1·00135	Axis error = +0·3
4	*18th September*	*Temperature* 21·0°C	*Relative humidity* 57%
	+1 g	+1·00119	$B_1 = +0·4$
	0	+0·00005	$B_2 = +0·1$
	−1 g	−1·00117	$B_2 - B_1 = -0·3$
	0	+0·00002	Scale factor = 1·00118
	+1 g	+1·00120	Axis error = +0·2

From this group of results it may be seen that, whilst parameters such as scale factor and bias alter with time, temperature and humidity, bias discrepancy and axis error remain constant to within the limits of measuring accuracy.

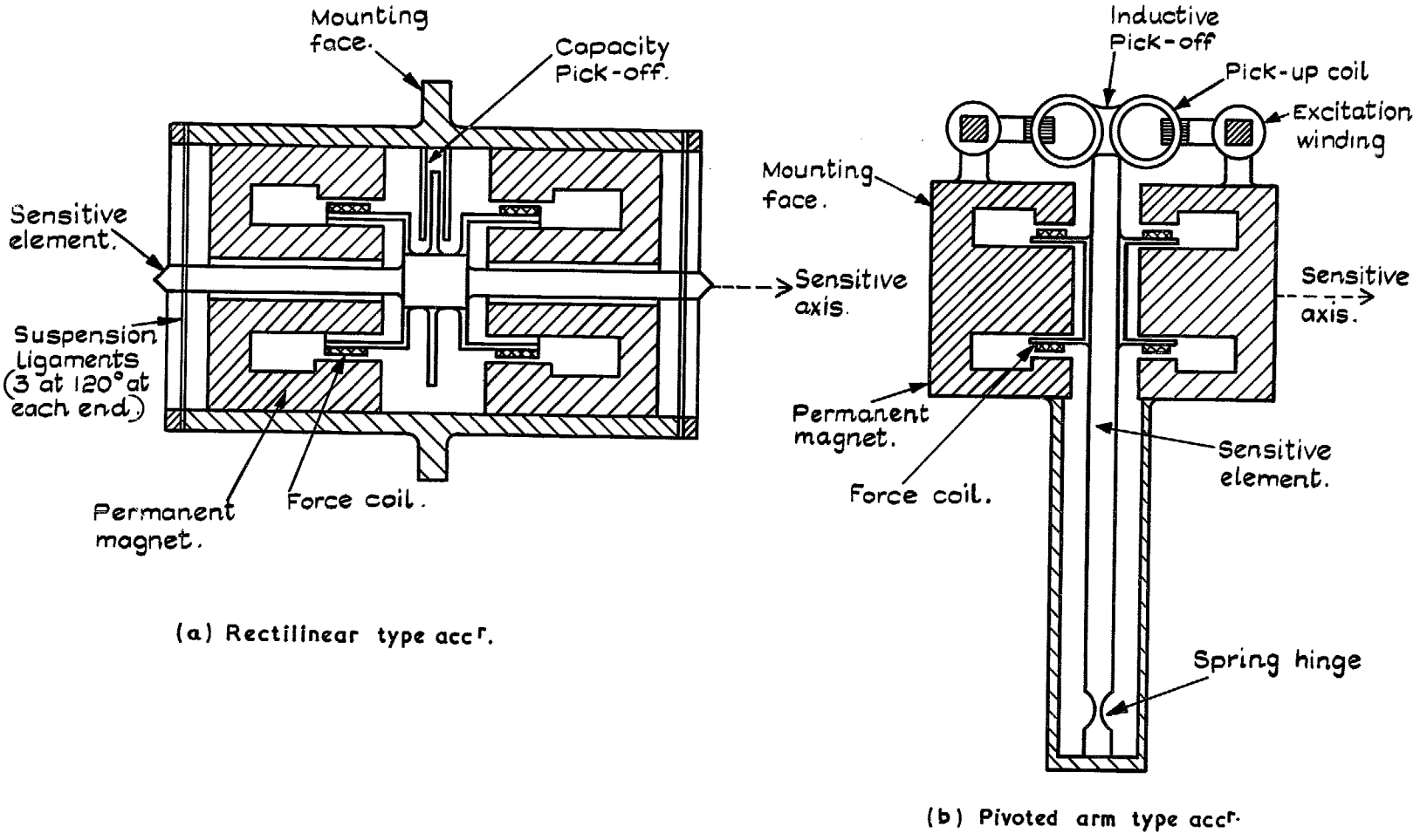

FIG. 1 a & b. Accelerometer schematic diagrams.

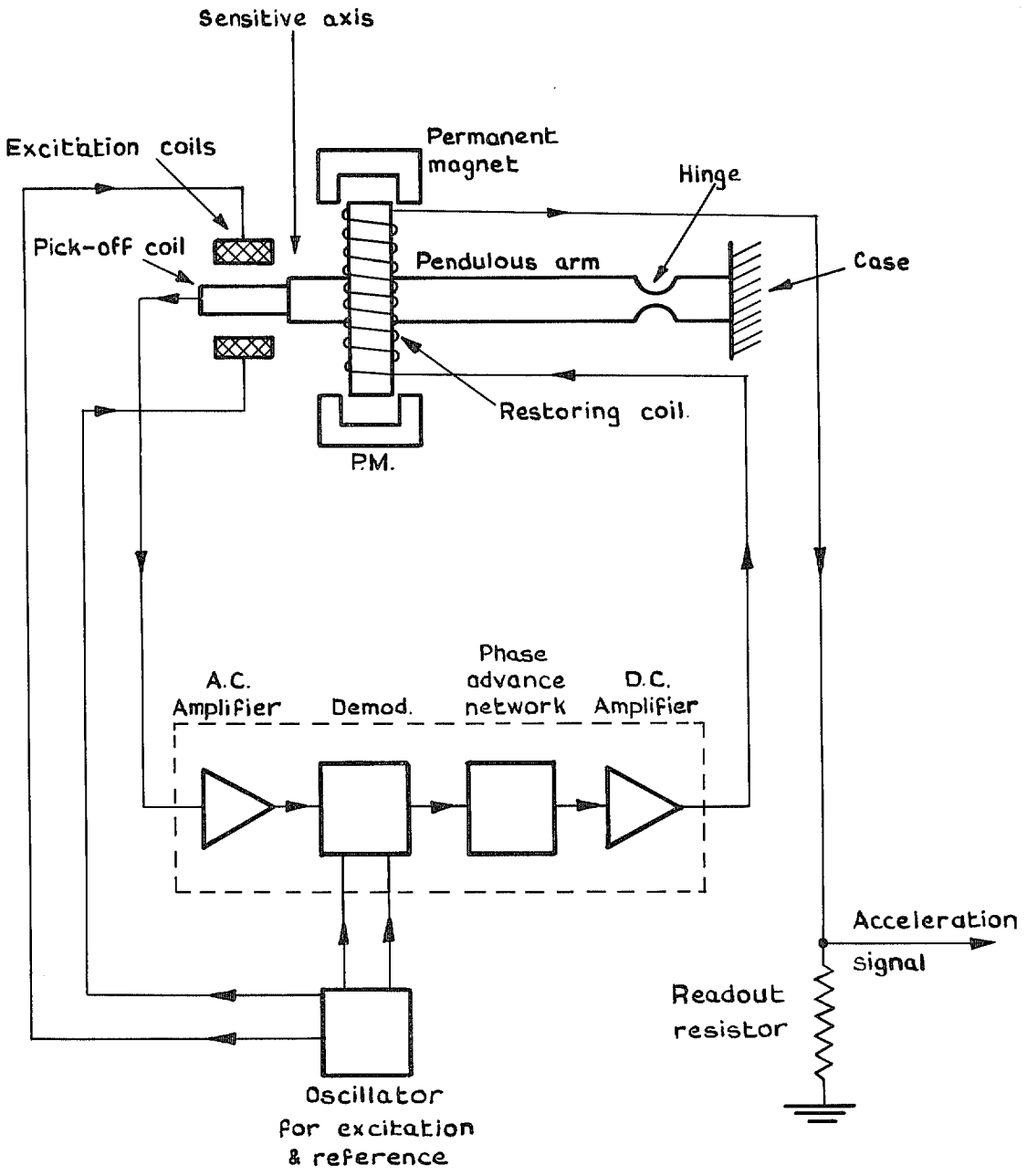

FIG. 2. Circuit of pivoted-arm type accelerometer.

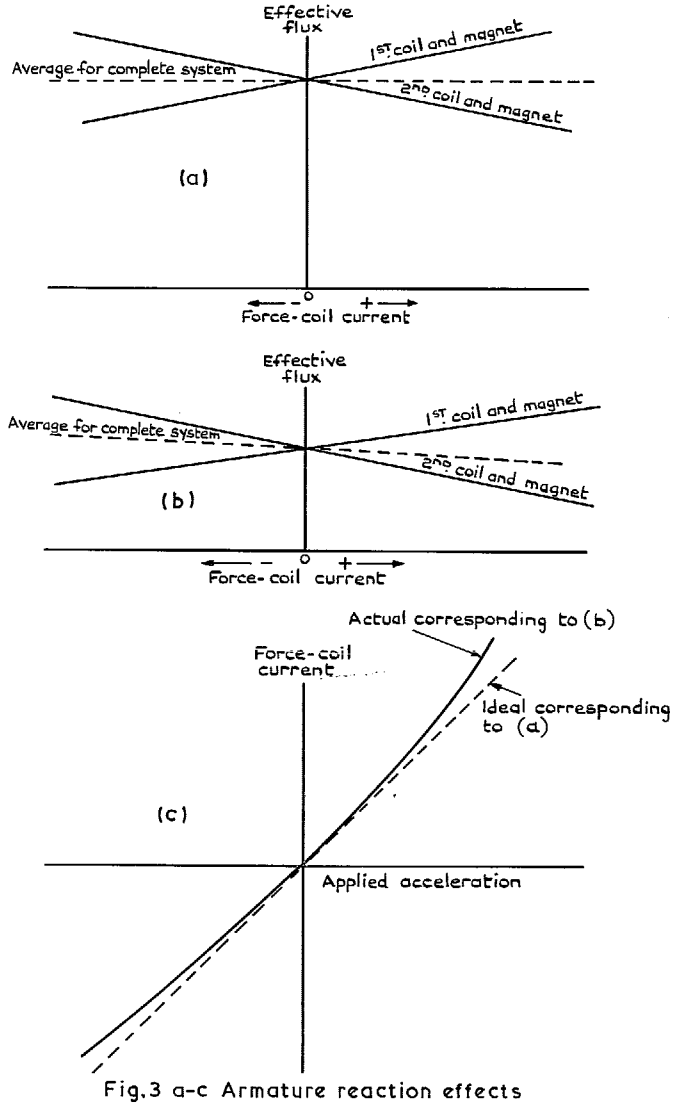

FIG. 3 a–c. Armature reaction effects.

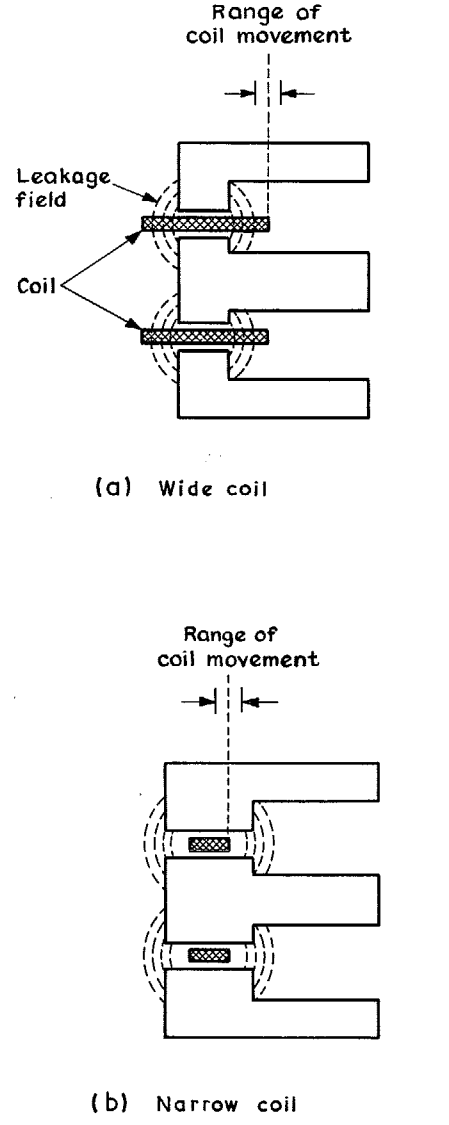

FIG. 4 a & b. Constancy of effective field.

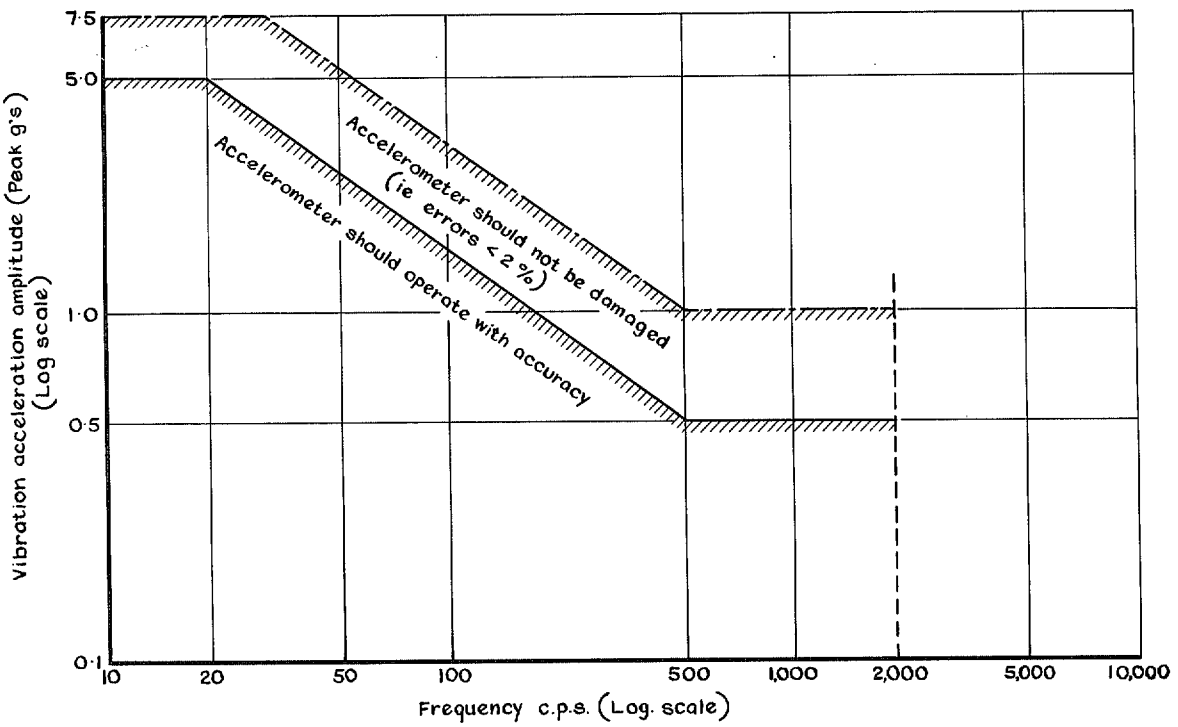

FIG. 5. Example of vibration spectrum.

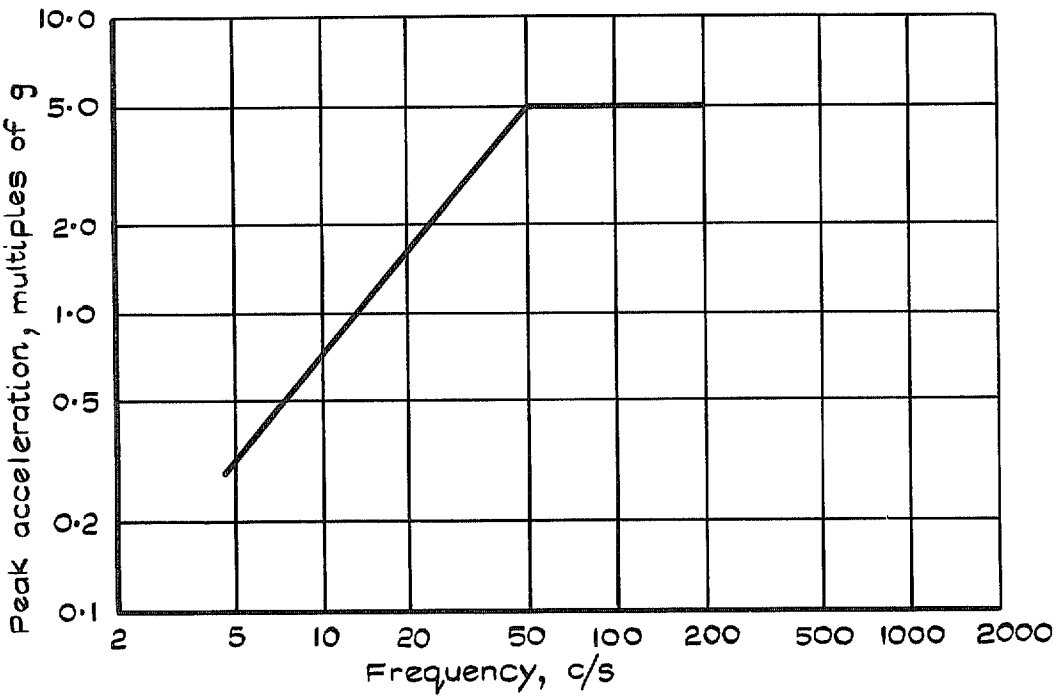

FIG. 6. Typical vibration spectrum.

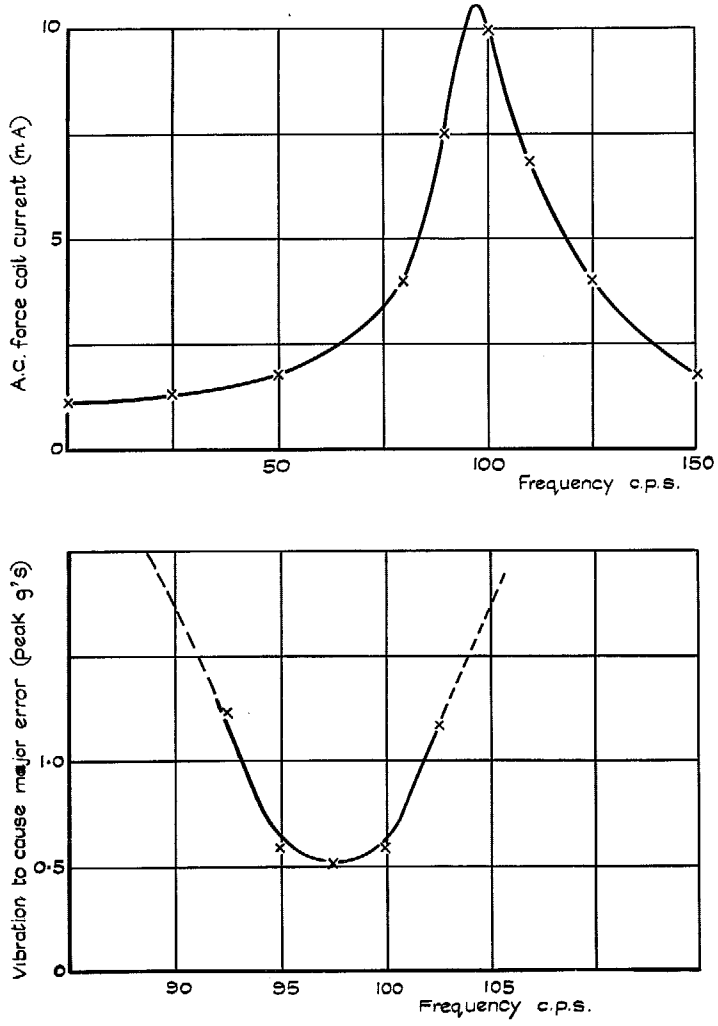

FIG. 7 a & b. Vibration tests results for an undamped, low-gain accelerometer system.

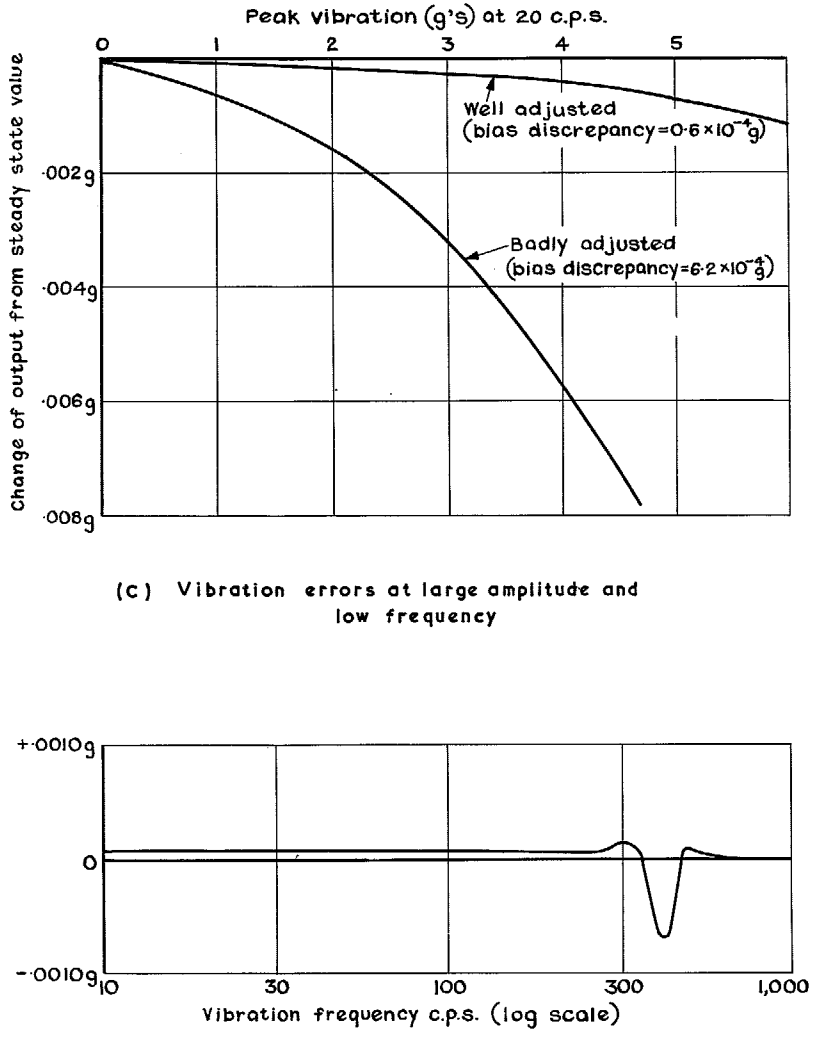

FIG. 7 c & d. Vibration test results.

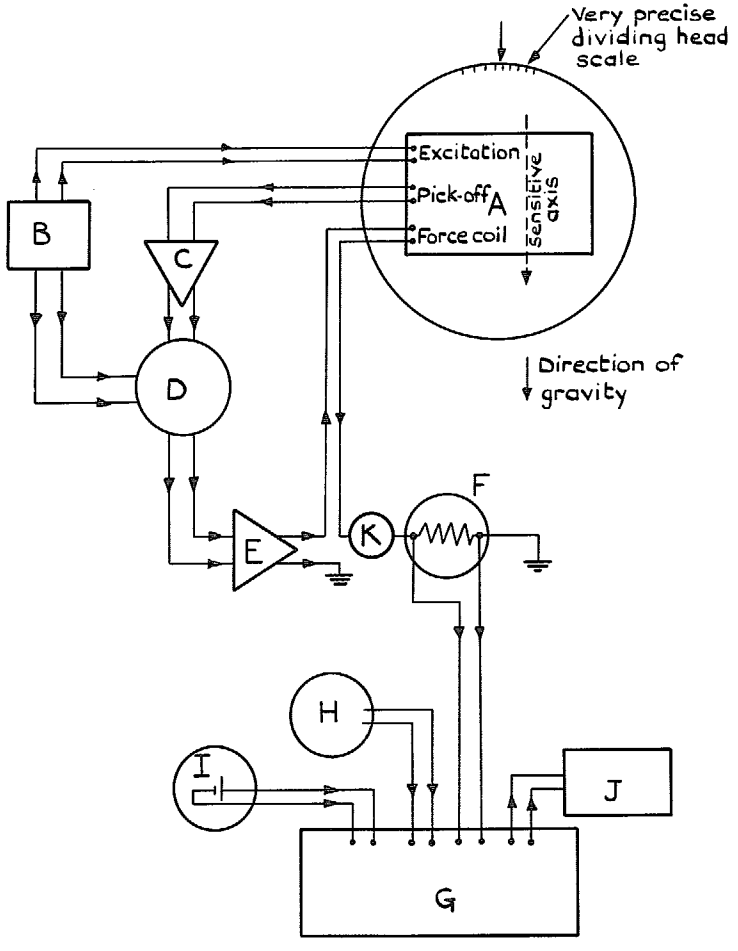

A – Accelerometer on dividing head
B – Oscillator
C – A.C. Amplifier
D – Phase sensitive rectifier
E – D.C. Amplifier (including stabilizing network)
F – Sub-standard resistance (read-out resistance) of known temperature coefficient
G – Potentiometer (accurate to 1 part in 10^5)
H – Weston standard cell (well lagged and with an accurate thermometer)
I – 2 volt wet cell
J – Galvanometer
K – Centre-zero or reversible D.C. milliameter

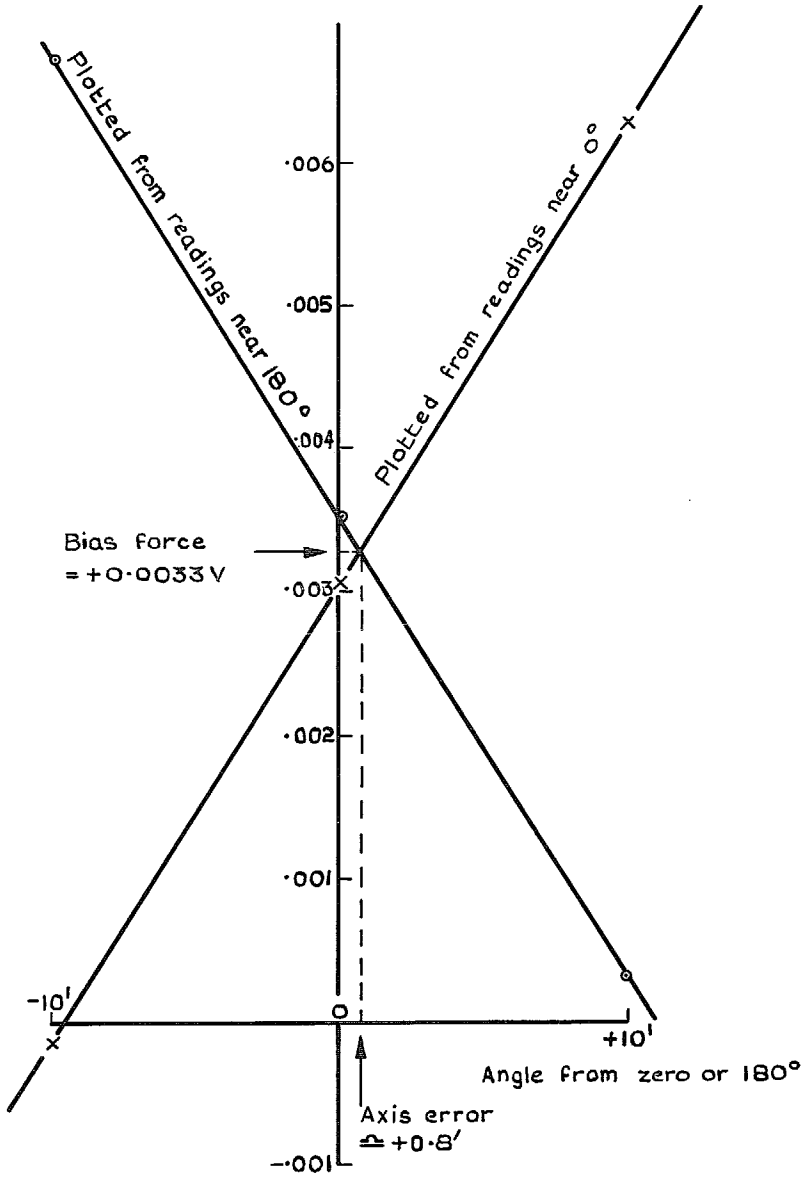

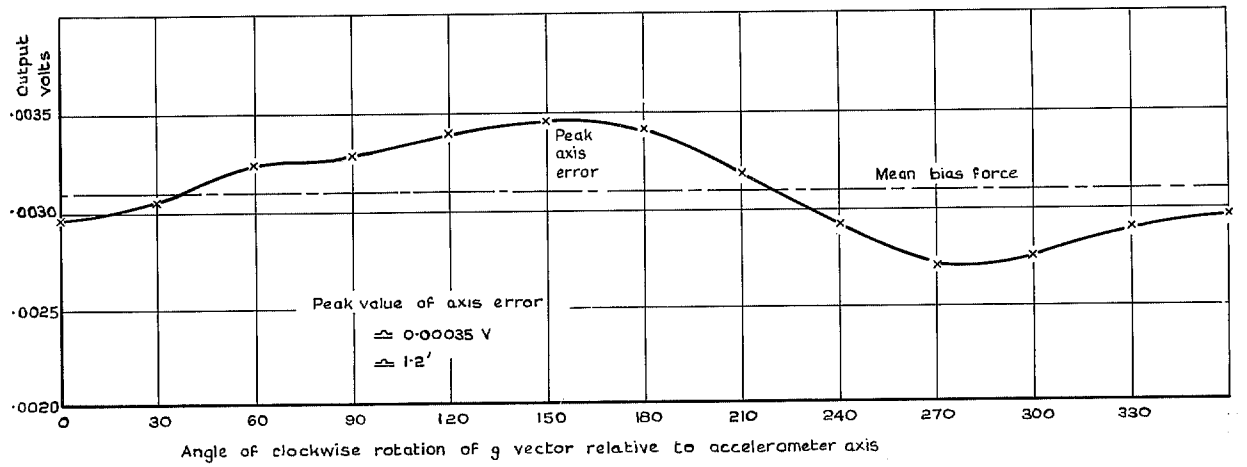

FIG. 10. Axis error test.

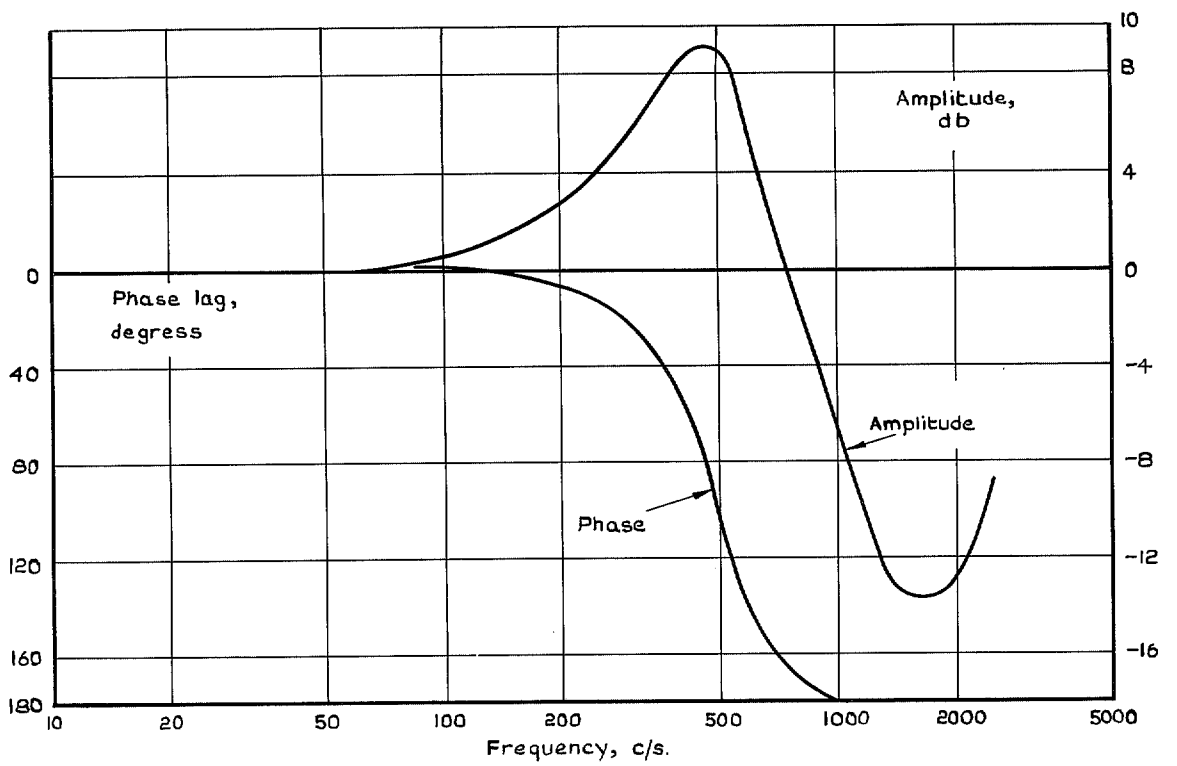

FIG. 11. Frequency response of air-filled accelerometer and associated circuits.

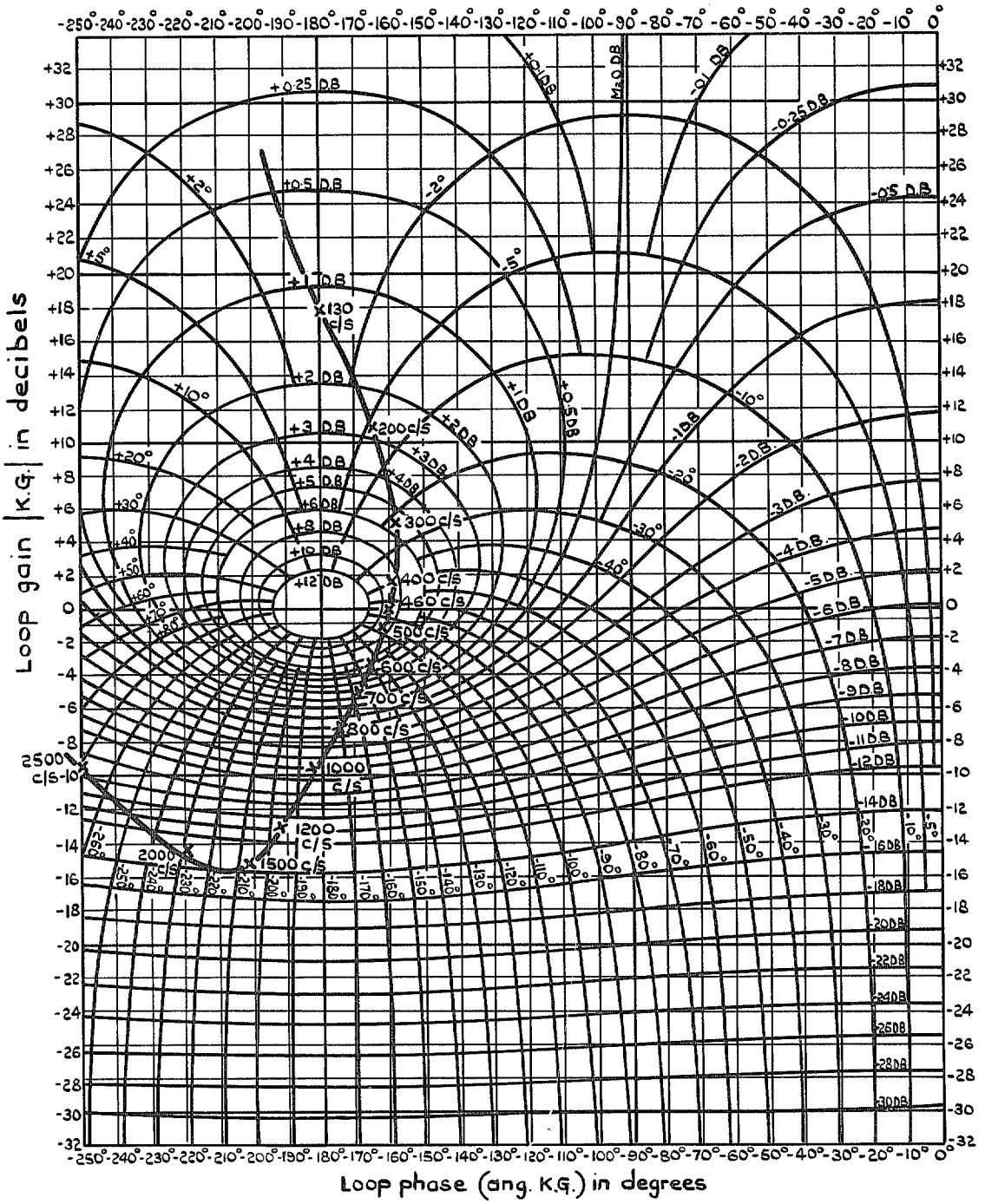

FIG. 12. Frequency response (Nichols diagram) of air-filled accelerometer and associated circuits.

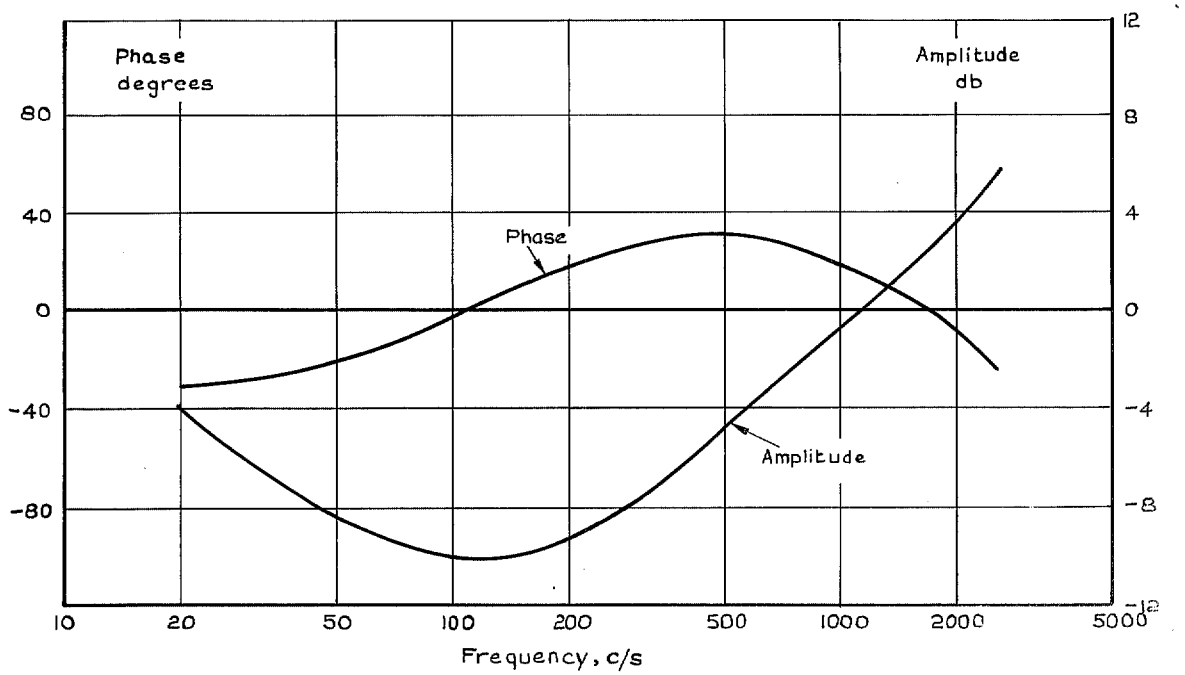

FIG. 13. Frequency response of amplifier (air-filled accelerometer).

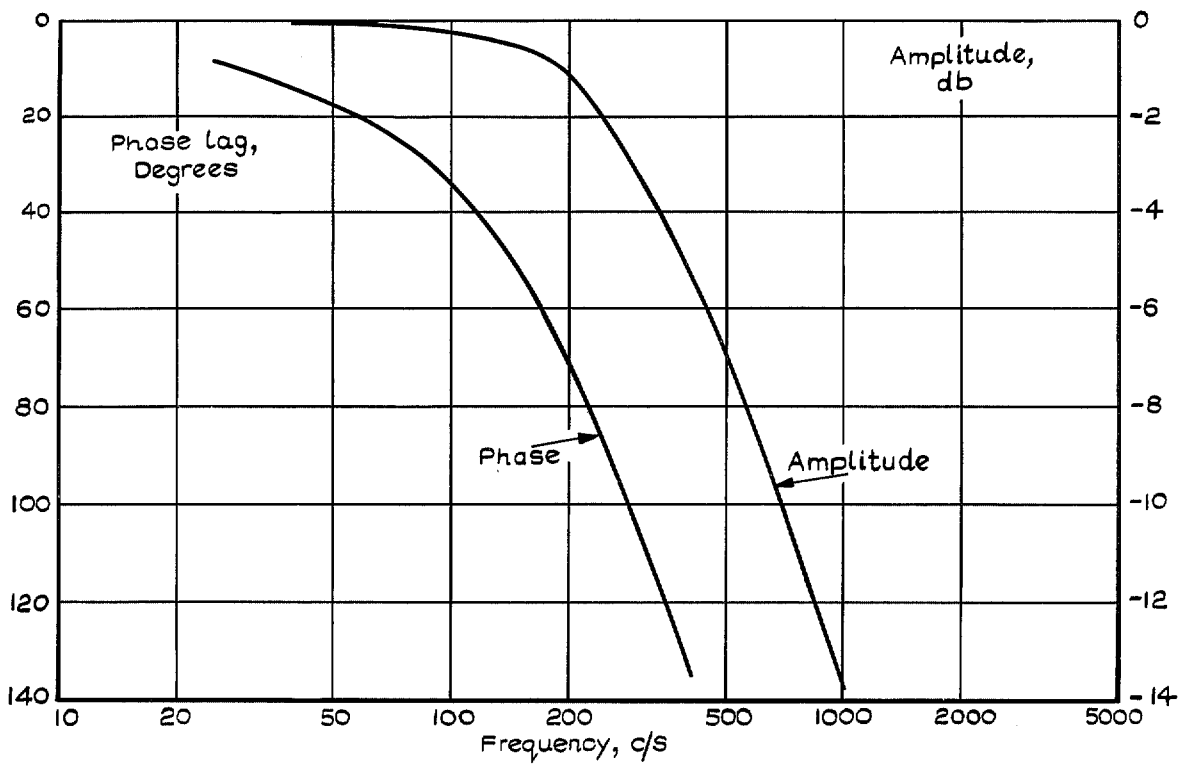

FIG. 14. Frequency response of oil-filled accelerometer and associated circuits.

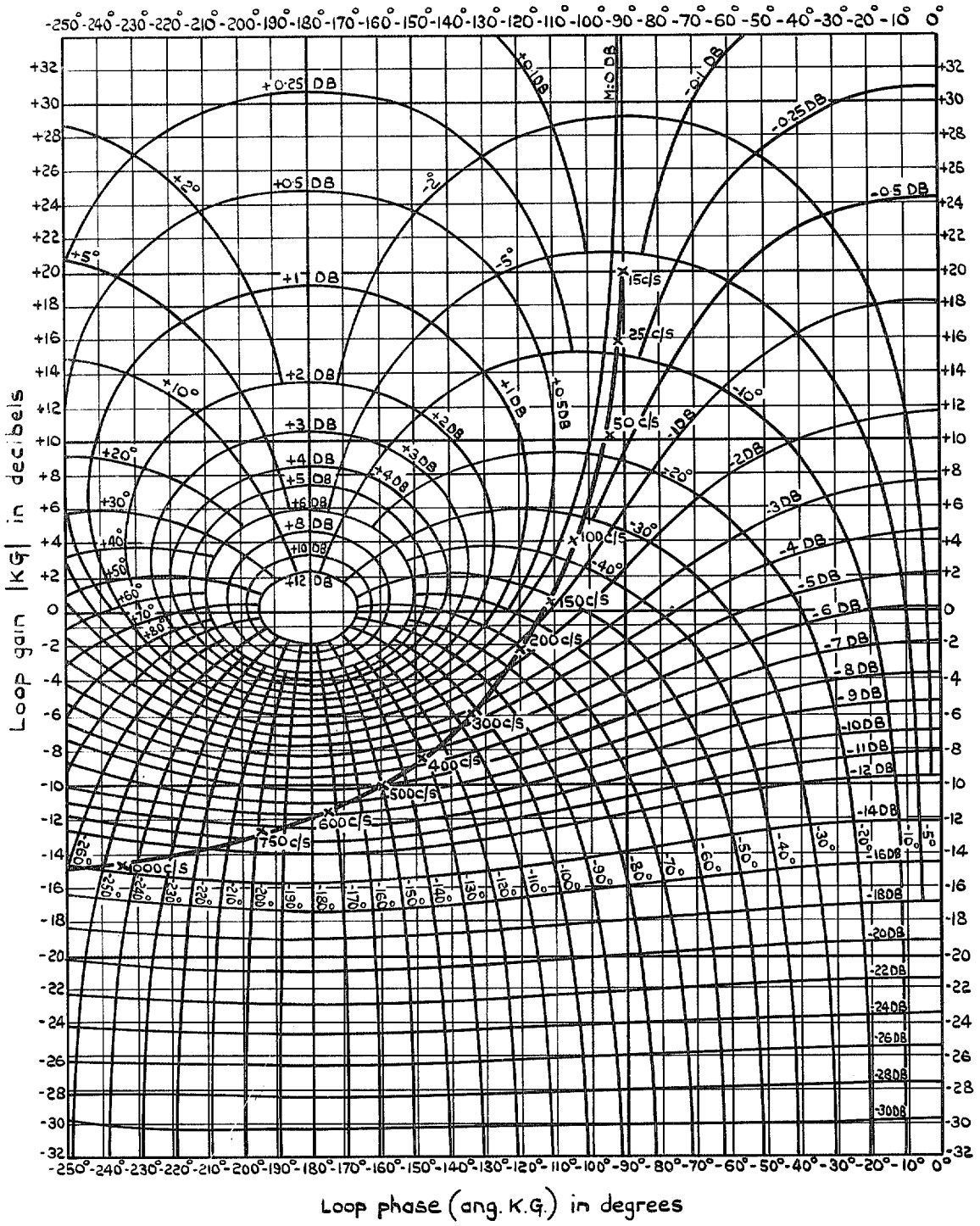

FIG. 15. Frequency response (Nichols diagram) of oil-filled accelerometer and associated circuits.

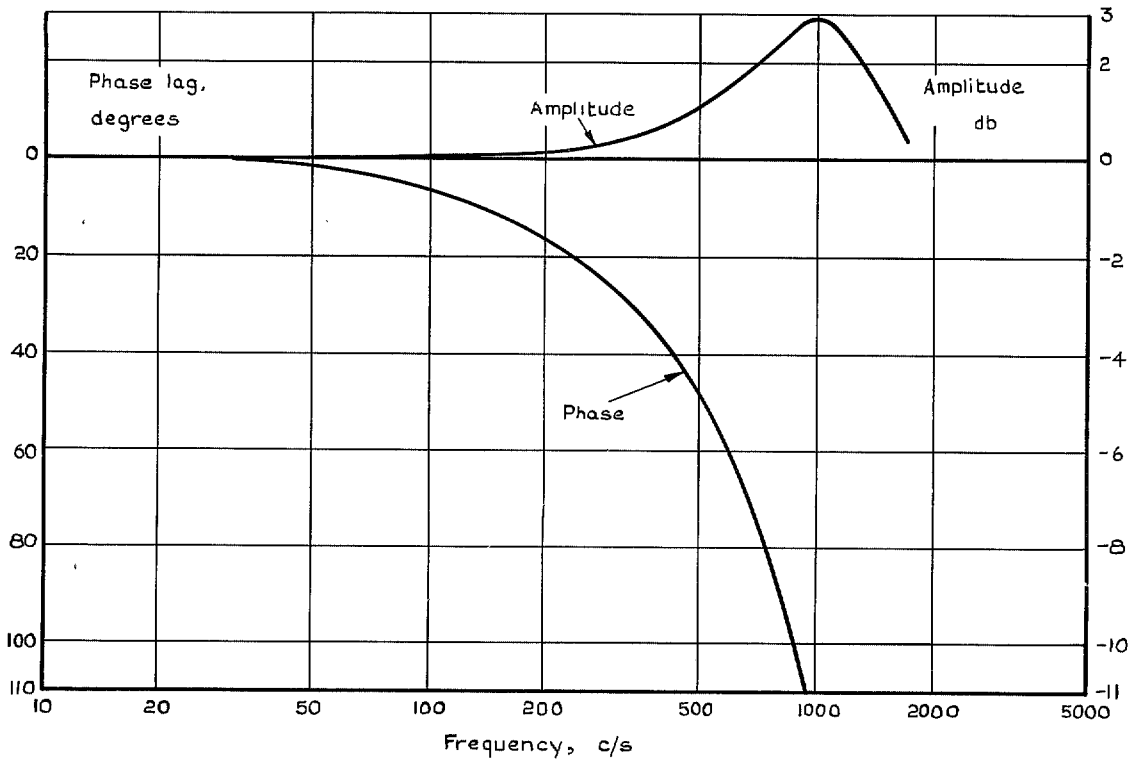

FIG. 16. Frequency response of amplifier (oil-filled accelerometer).

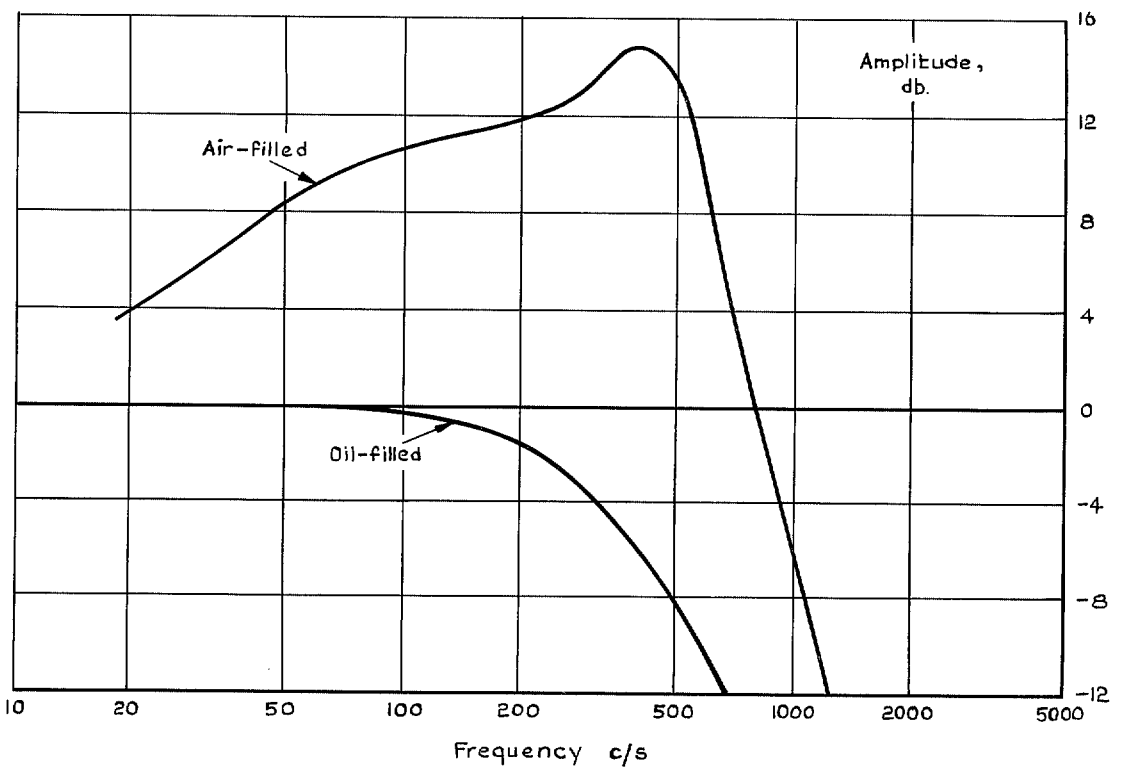

FIG. 17. Frequency response of sensitive element.

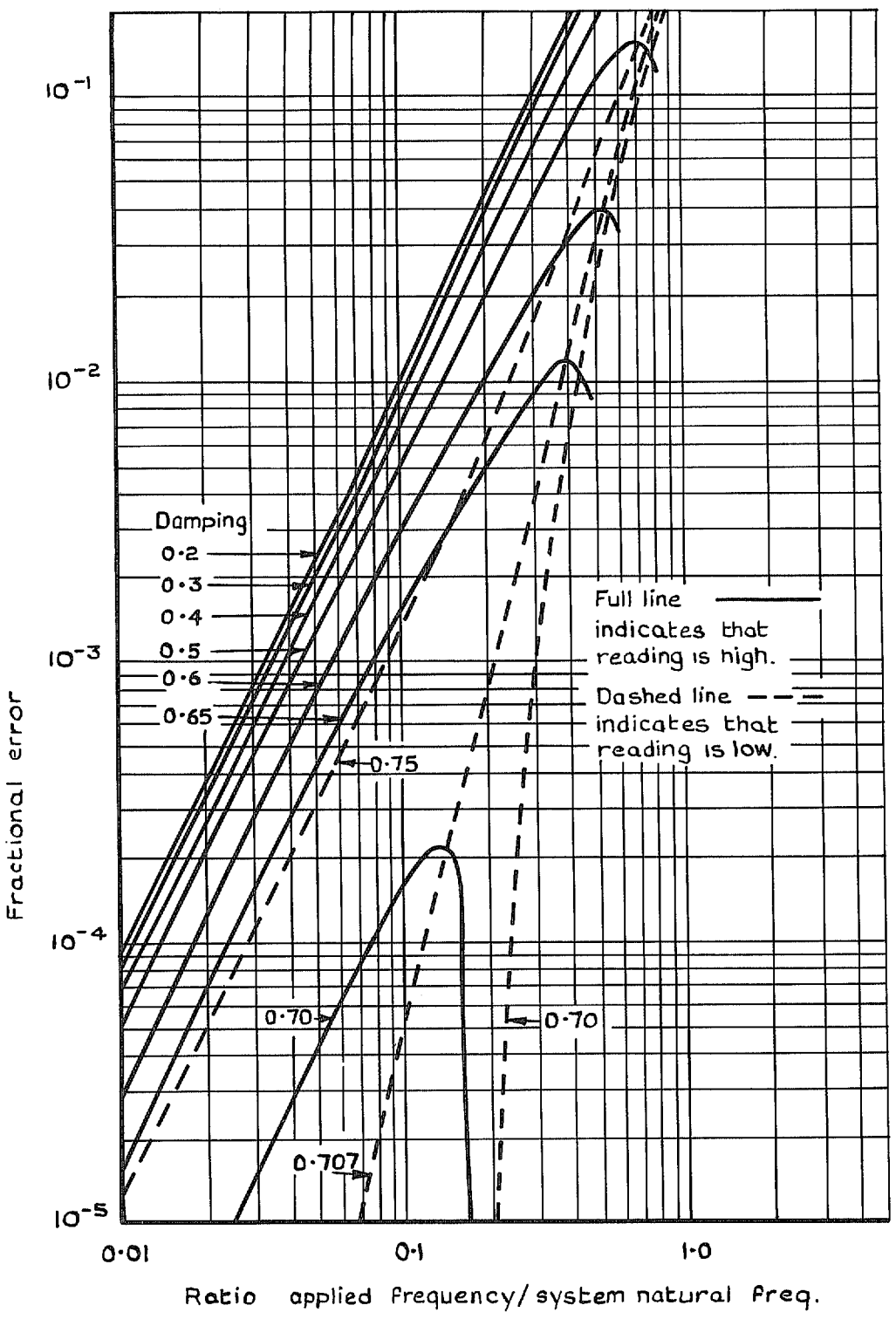

FIG. 18. Accelerometer used for measuring vibration fractional error due to frequency response.

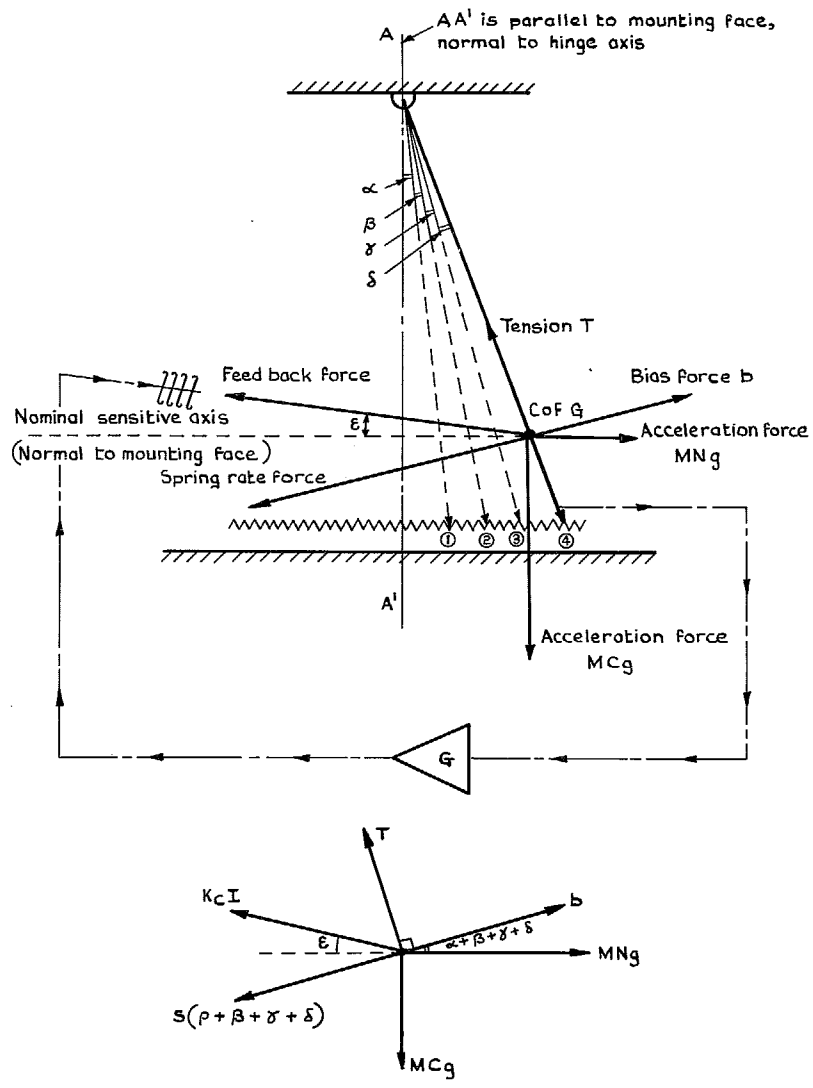

FIG. 19. Static operating conditions pivoted arm type accelerometer.

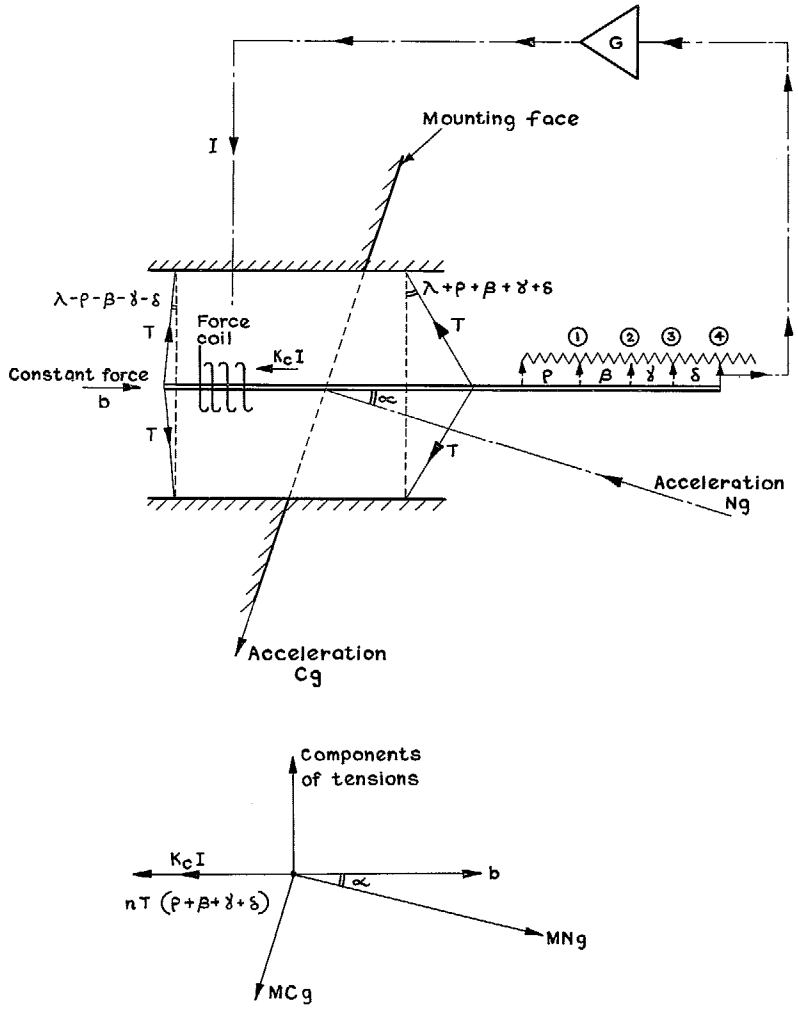

FIG. 20. Static operating conditions. Rectilinear type accelerometer.

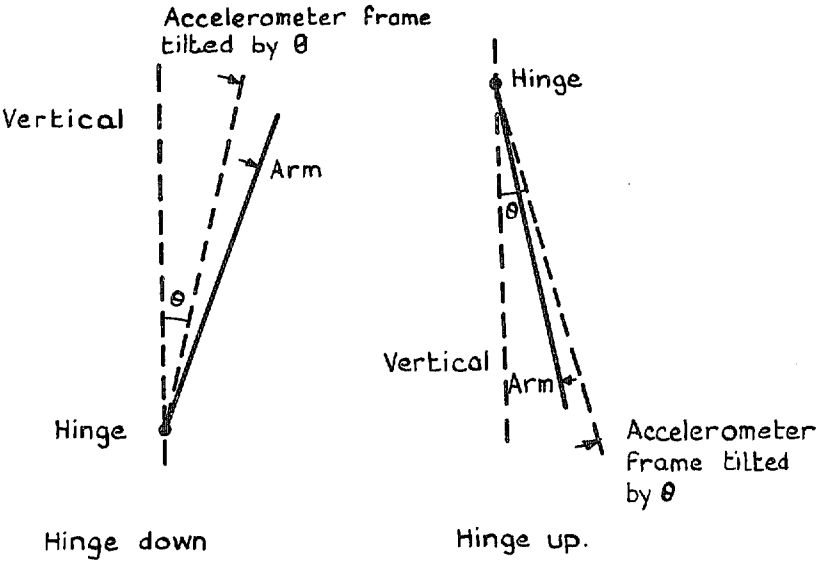

(a) Measurement of hinge stiffness and pick-off sensitivity

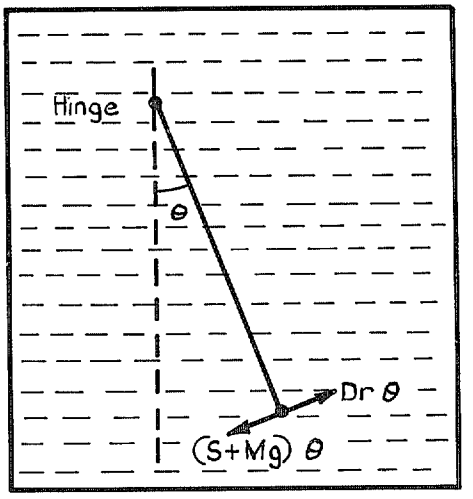

(b) Measurement of time-constant of oil—filled accelerometer

FIG. 21. Accelerometer open-loop tests.

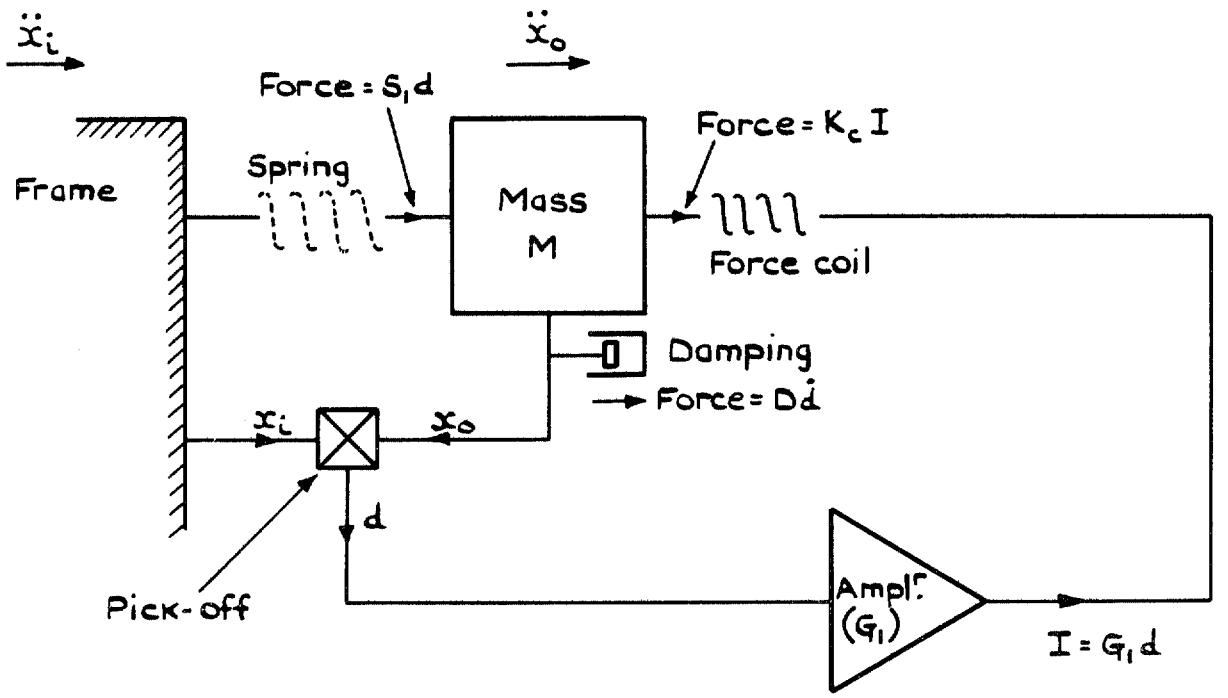

FIG. 22. Servo loop schematic.

Printed in Wales for Her Majesty's Stationery Office by Allens Printers (Wales) Limited

Dd. 146916 K.5.

Published by
HER MAJESTY'S STATIONERY OFFICE

To be purchased from
49 High Holborn, London WC1
13A Castle Street, Edinburgh EH2 3AR
109 St. Mary Street, Cardiff CF1 1JW
Brazennose Street, Manchester M60 8AS
50 Fairfax Street, Bristol BS1 3DE
258 Broad Street, Birmingham 1
7 Linenhall Street, Belfast BT2 8AY
or through any bookseller

R. & M. No. 3601

SBN 11 470236 5